NCU-HEP-k014
Feb 2004
rev. Aug 2004

Radiative B decays in Supersymmetry without R-parity

Otto C. W. Kong and Rishikesh D. Vaidya
Department of Physics, National Central University,
Chung-Li 32054 Taiwan.

We present a systematic analysis of all the contributions at the leading log order to the branching ratio of the inclusive radiative decay $B \to X_s + \gamma$ in the framework of supersymmetry without R-parity. The relevant set of four-quark operators involved in QCD running are extended from 6 (within SM and MSSM) to 24, with also many new contributions to the Wilson coefficients of (chromo)magnetic penguins for either chiral structure. We present complete analytical results here without any *a priori* assumptions on the form of R-parity violation. Mass eigenstate expressions are given, hence the results are free from the commonly adopted mass-insertion approximation. In the numerical analysis, we focus here only on the influence of the trilinear λ'_{ijk} couplings and report on the possibility of a few orders of magnitude improvement for the bounds on a few combinations of the λ' couplings. Our study shows that the Wilson coefficients of the current-current operators due to R-parity violation dominate over the direct contributions to the penguins. However, the inter-play of various contributions is complicated due to the QCD corrections which we elaborate here.

PACS numbers:

I. INTRODUCTION

With the successful testing of the gauge sector during the LEP era, the standard model (SM) of particle physics has certainly established itself as an essentially correct theory at and below the GeV scale. However, it still leaves many basic issues to be investigated. Even if one forgets about the hierarchy problem, and the need for neutrino masses, a cursory look at the error bars of about 20 % on the various flavor parameters [1], and their wide range of apparently arbitrary numerical values suggests that the flavor sector is still much of a misery. Within flavor physics, it is the phenomena of the flavor changing neutral currents (FCNCs) that could be the window of the physics beyond SM. Forbidden at the tree level due to the unitarity of $V_{\rm CKM}$, FCNCs are loop induced where exotic virtualities (from supersymmetry or otherwise) could pop up and hence completely change the predictions for the decay rate. This could prove to be complementary to the direct search of the exotic particles by hinting toward a particular class of models or by ruling out large regions in the parameter space of beyond SM models, and thus, guiding the accelerator searches.

Among the FCNCs, the process $B \to X_s + \gamma$ is particularly attractive, both theoretically as well as experimentally. From the point of view of theory, though the calculation is very complicated and was a major challenge due to the ambiguities following 'scheme dependence' of the decay rate right at the leading log (LL) [2, 3], it was worth an effort. Unlike many hadronic processes, it can largely be freed from the scale and scheme dependence within the framework of renormalization group improved perturbation theory and heavy mass expansion together with the assumption of quark-hadron duality. All this is possible because $m_b >> \Lambda_{QCD}$ and hence, the inclusive decay $B \to X_s + \gamma$ is very well approximated by the corresponding partonic level transition $b \to s + \gamma$ where the non-perturbative pathogens play only sub-leading role being suppressed by at least two powers of m_b (the corrections are less than 10%). The next to leading log (NLL) result for the branching fraction in the case of SM is given as [4, 5]:

$$Br\left[B \to X_s + \gamma\ (E_\gamma > 1.6GeV)\right]_{\rm SM} = (3.57 \pm 0.30) \times 10^{-4}\ . \tag{1}$$

Here, E_γ is the energy cut on the photon spectrum to get rid of the background photons. The above result implies that this particular 'rare' decay is actually not so rare. This is because, unlike other rare decays, where the rate is $\propto G_F^2 \alpha_{QED}^2$, here it is $\propto G_F^2 \alpha_{QED}$. Also due to the heavy top in the loop, GIM suppression is not much effective. The high rate has already been quite well measured by CLEO [6], BELLE [7] and ALEPH [8]. The results of different experiments are consistent with each other. A weighted average of the available experimental measurement is problematic, because the model dependence errors (and also the systematic errors) are correlated and differ within the various measurements. An analysis taking into account the correlations, leads to the following world average [9]

$$Br\left[B \to X_s + \gamma\ (E_\gamma > 1.6GeV)\right]_{\rm EXP} = (3.34 \pm 0.38) \times 10^{-4}\ . \tag{2}$$

Within 1σ it matches the SM predictions [4, 5]. So it is clear that there is not much room for new physics contributions[1]. Either the new physics contributions are negligible, or there are large cancellations among various contributions. Thus, a study of new physics contributions can help to reduce the viable regions in parameter space of the relevant model. This channel is indeed very well studied in the most popular theory of beyond SM physics, namely the minimal supersymmetric standard model (MSSM) [10, 11, 12]. There is already a vast literature on the topic and we are not adding to that here. The imposed baryon number (B) and lepton number (L) conservation (in the form of R-parity) within MSSM, is totally *ad hoc*. It is an overkill of a problem of proton decay which can be easily rescued by alternatives like baryon parity. It also forbids the neutrino masses that would otherwise arise naturally. In fact, supersymmetrizing the SM with its sacred gauge symmetries and renormalizability, one naturally lands into the generic supersymmetric standard model or the supersymmetry (SUSY) without R-parity [13]. However, due to the presence of a large number of free parameters, any phenomenological study of R-parity violation (RPV) models is a daunting task. On the other hand, one may consider the origin and suppression of these parameters as due to a spontaneously broken anomalous Abelian family symmetry which is invoked to understand the fermion mass hierarchies [14]. In ref.[15] such an attempt is made to understand the pattern of R-parity violation consistent with phenomenology at the electroweak scale. However, in the absence of a compelling model of the kind, it is imperative that all possible phenomenological constraints on these,*a priori*, free parameters be studied. Such complexity necessitates a careful examination of the exact definition of the RPV couplings, and the choice of an optimal parametrization of the latter, or rather the full model Lagrangian, that can simplify the structure of mass matrices to enable an analytical diagonalization in a suitable approximation. The single vev parametrization (SVP), first explicitly advocated in [17] is such a parametrization. In this paper, we investigate the RPV contributions from the generic model to the process

[1] See the note added in proof at the end.

$b \to s + \gamma$ within the framework of SVP [16]. We give analytical formulae that include all possible contributions without *a priori* assumption on the form of R-parity violation. In the same spirit as an earlier study on $\mu \to e + \gamma$ [18], we give mass eigenstate expressions, hence free from the commonly adopted mass-insertion approximation. In the numerical analysis, we focus in this paper only on the influence of the trilinear λ'_{ijk} couplings and report on the possibility of a few orders of magnitude improvement for the bounds on a few combination of λ'_{ijk} parameters. Our formulation also has the advantage that the physical meaning of the λ'-couplings would not change at all, whether the numerical values of any of the other RPV parameters are vanishingly small or otherwise.

There have been some studies on the process within the general framework of R-parity violation. More systematic analysis are exemplified by refs.[19, 20]. Ref.[19], fails to consider the additional 18 four-quark operators which, in fact, give the dominant contribution in most of the cases. As we shall demonstrate, the interplay of various contributions along with the QCD corrections, is very complicated and hence various contributions could add up or cancel depending on a particular case. The more recent work of ref.[20] has considered a complete operator basis. However, we find their formula for Wilson coefficient incomplete, and they do not report on the possibility of a few orders of magnitude improvement on the bounds for certain combinations of RPV couplings, as we present here. We must mention here that around the same time as ref.[20] authors of ref.[21] published an analysis of the CP-asymmetries in the radiative B-decays, which involved a similar calculation machinery with the extended operator basis. To the best of our knowledge all the available studies on the topic in the literature, in fact are incomplete or incorrect to some extent. This is mostly a problem of incomplete consideration for the RPV couplings of the bilinear type and the mass mixings the latter produce in the sectors of fermions and scalars. We present here a complete treatment of the full operator basis together with the corresponding Wilson coefficients under the truly generic and consistent formulation of SUSY without R-parity. In fact, the existence of interesting contributions from combinations of bilinear and trilinear RPV couplings in the process has been noted in the earlier studies of the model under the SVP formulation [22, 23]. We present the full analytical result here. However, due to other complications involved, we will postpone any numerical study on the aspect to a later publication. Focusing our attention here on the trilinear RPV parameters, we perform our analysis at the leading log order. Such an approximation entails uncertainties of about 25 %. However, owing to sensitive dependence of the result on the large number of input parameters, we consider it worth-while to examine the relevant parameter space and obtain order of magnitude bounds before performing any precision analysis.

The paper is organized as follows: In section II we briefly summarize the main features of SVP parametrization and also set our notation. Section III deals with the effective Hamiltonian formulation, the extended operator basis and the Wilson coefficients. Section IV discusses the decay rate calculation in relation to the anomalous dimension matrix and the renormalization group running of the full set of 28 operators. We discuss our major numerical results in section V, and conclude the paper after. Some details involving the full set of 28 operators and the 28×28 anomalous dimension matrix is left to an appendix. The numerical results discussed here are restricted to those obtained from combinations trilinear couplings along. Contributions from combinations of a trilinear and a bilinear parameter, the latter going into the loop diagrams through RPV mass mixings, form another class of novel results essentially not studied before. We present that latter part, from our parallel study, in an independent publication[24].

II. THE SINGLE VEV PARAMETRIZATION

The most general renormalizable superpotential for the generic supersymmetric SM (without R-parity) can be written as

$$W{=}\varepsilon_{ab}\Big[\mu_\alpha \hat{H}_u^a \hat{L}_\alpha^b + h_{ik}^u \hat{Q}_i^a \hat{H}_u^b \hat{U}_k^C + \lambda'_{\alpha jk} \hat{L}_\alpha^a \hat{Q}_j^b \hat{D}_k^C + \frac{1}{2}\lambda_{\alpha\beta k} \hat{L}_\alpha^a \hat{L}_\beta^b \hat{E}_k^C\Big] + \frac{1}{2}\lambda''_{ijk} \hat{U}_i^C \hat{D}_j^C \hat{D}_k^C \ , \tag{3}$$

where (a, b) are $SU(2)$ indices, (i, j, k) are the usual family (flavor) indices, and (α, β) are the extended flavor indices going from 0 to 3. In the limit where $\lambda_{ijk}, \lambda'_{ijk}, \lambda''_{ijk}$ and μ_i all vanish, one recovers the expression for the R-parity preserving case, with $\hat{L}_0$ identified as $\hat{H}_d$. Without R-parity imposed, the latter is not *a priori* distinguishable from the $\hat{L}_i$'s. Note that λ is antisymmetric in the first two indices, as required by the $SU(2)$ product rules, as shown explicitly here with $\varepsilon_{12} = -\varepsilon_{21} = 1$. Similarly, λ'' is antisymmetric in the last two indices, from $SU(3)_C$. R-parity is exactly an *ad hoc* symmetry put in to make $\hat{L}_0$, stand out from the other $\hat{L}_i$'s as the candidate for $\hat{H}_d$. It is defined in terms of baryon number, lepton number, and spin as, explicitly, $\mathcal{R} = (-1)^{3B+L+2S}$. The consequence is that the accidental symmetries of baryon number and lepton number in the SM are preserved, at the expense of making particles and super-particles having a categorically different quantum number, R-parity. As mentioned above, R-parity hence kills the dangerous proton decay but also forbids neutrino masses within the model.

After the supersymmetrization of the SM, however, some of the superfields lose the exact identities they have in relation to the physical particles. The latter have to be mass eigenstates, which have to be worked out from the

Lagrangian of the model. Assuming electroweak symmetry breaking, we have now five (color-singlet) charged fermions, for example. There are also 1+4 VEV's admitted, together with a SUSY breaking gaugino mass. If one writes down naively the (tree-level) mass matrix, the result is extremely complicated with all the μ_α and $\lambda_{\alpha\beta k}$ couplings involved, from which the only definite experimental data are the three physical lepton masses as the light eigenvalues, and the overall magnitude of the electroweak symmetry breaking VEV's. The task of analyzing the model seems to be formidable.

Doing phenomenological studies without specifying a choice of flavor bases is, however, ambiguous. It is like doing SM quark physics with 18 complex Yukawa couplings, instead of the 10 real physical parameters. As far as the SM itself is concerned, the extra 26 real parameters are simply redundant, and attempts to relate the full 36 parameters to experimental data will be futile. In the case at hand, the choice of an optimal parametrization mainly concerns the 4 $\hat{L}_\alpha$ flavors. In the single vev parametrization[17] (SVP), flavor bases are chosen such that : 1) among the $\hat{L}_\alpha$'s, only $\hat{L}_0$, bears a VEV, *i.e.* $\langle \hat{L}_i \rangle \equiv 0$; 2) $y^e_{jk} (\equiv \lambda_{0jk}) = \frac{\sqrt{2}}{v_0} \,\mathrm{diag}\{m_1, m_2, m_3\}$; 3) $y^d_{jk} (\equiv \lambda'_{0jk} = -\lambda_{j0k}) = \frac{\sqrt{2}}{v_0} \,\mathrm{diag}\{m_d, m_s, m_b\}$; 4) $h^u_{ik} = \frac{\sqrt{2}}{v_u} V^T_{\rm CKM} \,\mathrm{diag}\{m_u, m_c, m_t\}$, where $v_0 \equiv \sqrt{2}\,\langle \hat{L}_0 \rangle$ and $v_u \equiv \sqrt{2}\,\langle \hat{H}_u \rangle$. Thus, the parametrization singles out the $\hat{L}_0$ superfield as the one containing the Higgs. As a result, it gives the complete RPV effects on the tree-level mass matrices of all the states (scalars and fermions) the simplest structure. The latter is a strong technical advantage.

The soft SUSY breaking part of the Lagrangian can be written as

$$\begin{aligned} V_{\rm soft} \;=\; & \tilde{Q}^\dagger \tilde{m}^2_Q \,\tilde{Q} + \tilde{U}^\dagger \tilde{m}^2_U \,\tilde{U} + \tilde{D}^\dagger \tilde{m}^2_D \,\tilde{D} + \tilde{L}^\dagger \tilde{m}^2_L \tilde{L} + \tilde{E}^\dagger \tilde{m}^2_E \,\tilde{E} + \tilde{m}^2_{H_u} \,|H_u|^2 + \Big[\frac{M_1}{2} \tilde{B}\tilde{B} + \frac{M_2}{2} \tilde{W}\tilde{W} \\ & + \frac{M_3}{2} \tilde{g}\tilde{g} + \epsilon_{ab} \Big(B_\alpha \, H^a_u \tilde{L}^b_\alpha + A^U_{ij} \, \tilde{Q}^a_i H^b_u \tilde{U}^C_j + A^D_{ij} H^a_d \tilde{Q}^b_i \tilde{D}^C_j + A^E_{ij} H^a_d \tilde{L}^b_i \tilde{E}^C_j + A^{\lambda'}_{ijk} \tilde{L}^a_i \tilde{Q}^b_j \tilde{D}^C_k \\ & + \frac{1}{2} \, A^\lambda_{ijk} \tilde{L}^a_i \tilde{L}^b_j \tilde{E}^C_k \Big) + \frac{1}{2} \, A^{\lambda''}_{ijk} \tilde{U}^C_i \tilde{D}^C_j \tilde{D}^C_k + \text{h.c.} \Big] \,, \end{aligned} \tag{4}$$

where we have separated the R-parity conserving A-terms from the RPV ones (recall $\hat{H}_d \equiv \hat{L}_0$). Note that $\tilde{L}^\dagger \tilde{m}^2_{\tilde{L}} \tilde{L}$, unlike the other soft mass terms, is given by a 4×4 matrix. Explicitly, $\tilde{m}^2_{L_{00}}$ corresponds to $\tilde{m}^2_{H_d}$ of the MSSM case while $\tilde{m}^2_{L_{0k}}$'s give RPV mass mixings. Going from here, it is straight forward to obtain the squark and slepton masses. No RPV A-term enters the mass matrices for instance. Full matrices have been worked out, together with various diagonalizing matrix elements from the perturbative approximations for the matrices within the experimentally viable setting of small RPV couplings. Readers are referred to ref.[13] for further details.

III. THE EFFECTIVE HAMILTONIAN

A. The basic Strategy

The partonic transition $b \to s + \gamma$ is described by the magnetic penguin diagram (see Fig.1). QCD corrections are obtained by attaching a gluon line to the quarks lines. Such a correction forms a power series in $\alpha_{\rm QCD}\,(M_W) \ln(M^2_W/m^2_b) \sim 0.7$ which is too large to be treated in the perturbation framework. This can be efficiently handled within the framework of operator product expansion (OPE) and the renormalization group (RG) improved perturbation theory [25]. One writes down the effective Hamiltonian ($\mathcal{H}_{\rm eff}$) as a series of local operators $\mathcal{Q}_i(\mu)$ multiplied by the corresponding Wilson coefficients $C_i(\mu)$. Both, the operators and the Wilson coefficients are function of the scale μ, however, the effective Hamiltonian is expected to be scale independent. Thus, we can write

$$\mathcal{H}_{\rm eff} \;=\; \sum_i \, C_i(\mu) \, \mathcal{Q}_i(\mu) \;. \tag{5}$$

The choice of scale μ is arbitrary, and separates high scale physics ($> \mu$) and the low scale ($< \mu$). It is typically taken to be the mass scale of the decaying particle (in this case the b-quark). There are three major steps in the evaluation of the decay rate. They are:

- **Matching at M_W:** C_i are first evaluated perturbatively at the scale at which one decouples the heavy modes (say at $\mu = M_W$). This is done by imposing the equality of the effective, and the underlying theory Green functions, at external momenta that are much smaller than the masses of the decoupled particles.

- **Resummation:** Since the theory contains two disparate scales m_b and M_W, the large logarithms need to be resumed using RG improved perturbation theory. The RG equation for the C_i are given as:

$$\frac{dC_i}{dln\mu} = \gamma_{ji} C_j \;. \tag{6}$$

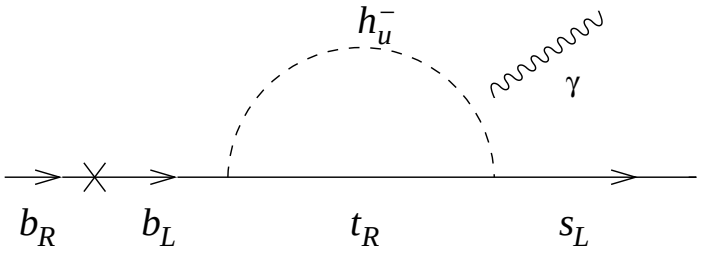

FIG. 1: Magnetic penguin diagram with Higgs in the loop. Here the chirality flip is on the external b-quark. Note that the photon can be attached to any electrically charged particle inside the loop but not outside the loop. Diagram with a photon outside the loop does not contribute to the magnetic transition. There are similar diagrams with other SUSY particles in the loop. For the chromo-magnetic penguin one attaches a gluon, instead of a photon to the quarks in the loop.

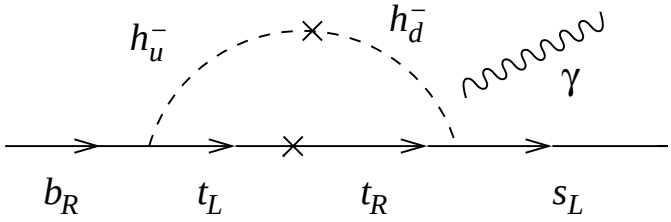

FIG. 2: A magnetic penguin digram but with the chirality flip inside the loop.

Here γ_{ji} is the anomalous dimension matrix (ADM). It is obtained from the ultra-violet (UV) divergences in the theory. The derivation of ADM is the most difficult part of the calculation. Solving the RG equation one gets the C_i at the scale m_b. Note that in our case the resummation is performed at the LL order.

- **Matrix elements:** Having obtained the $C_i(m_b)$ one finds the hadronic matrix elements of the relevant operators $\langle \mathcal{Q}_i \rangle$. Typically this involves some non-perturbative method; but in case of inclusive B decays, non-perturbative corrections are sub-leading and one can approximate the decay by a corresponding partonic level transition.

B. The Operators

Having outlined the strategy, let us list the army of operators beginning with the SM [2]. So far as one neglects the QCD corrections, the relevant operator is the magnetic penguin. However, once the penguin is dressed with the gluonic lines, it mixes with other current-current and QCD-penguin operator. They are given as:

$$\mathcal{Q}_{1,2} = (\bar{s}_{L\alpha}\,\gamma^\mu\,b_{L\alpha,\beta})\;(\bar{c}_{L\beta}\,\gamma_\mu\,c_{L\beta,\alpha})\;, \tag{7}$$

$$\mathcal{Q}_{3,4} = (\bar{s}_{L\alpha}\,\gamma^\mu\,b_{L\alpha,\beta})\sum_{i=u,c,d,s,b}(\bar{q}_{Li\beta}\,\gamma_\mu\,q_{Li\beta\alpha})\;, \tag{8}$$

$$\mathcal{Q}_{5,6} = (\bar{s}_{L\alpha}\,\gamma^\mu\,b_{L\alpha,\beta})\sum_{i=u,c,d,s,b}(\bar{q}_{Ri\beta}\,\gamma_\mu\,q_{Ri\beta,\alpha})\;, \tag{9}$$

$$\mathcal{Q}_7 = \frac{e}{16\pi^2}\,m_b\,\bar{s}_{L\alpha}\,\sigma_{\mu\nu}\,b_{R\alpha}\,F^{\mu\nu}\;, \tag{10}$$

$$\mathcal{Q}_8 = \frac{g_s}{16\pi^2}\,m_b\,\bar{s}_{L\alpha}\,\sigma_{\mu\nu}\,b_{R\beta}\,t^{a\alpha\beta}G^{a\mu\nu}\;. \tag{11}$$

Here, we have used Fierz re-ordering to write the first two operators. α and β are the colour indices and t^a are the generators of $SU(3)$. Other notations are self explanatory. Operators $\mathcal{Q}_3$ to $\mathcal{Q}_6$ are the QCD penguins, and $\mathcal{Q}_{7,8}$ are the magnetic and the chromomagnetic penguins respectively involving up-type quark and W-boson. We would like to remark here that for a novice there is some chance of confusion regarding the choice of operator basis. The above mentioned operator basis is arrived at by considering the external states on-shell and hence these cannot be transformed into each other using equations of motion [26]. In an off-shell calculation one must consider additional

operators [2]. Even for the on-shell basis there exist one more basis choice in the literature introduced by the authors of [28] [3].

Since the magnetic penguins are chirality flipping operators, they are necessarily proportional to the fermionic mass term. In principle one can also write down the following two operators obtained by flipping the chirality of $\mathcal{Q}_{7,8}$.

$$\widetilde{\mathcal{Q}}_7 = \frac{e}{16\pi^2}\, m_s\, \bar{s}_{R\alpha}\, \sigma_{\mu\nu}\, b_{L\alpha}\, F^{\mu\nu}\ , \tag{12}$$

$$\widetilde{\mathcal{Q}}_8 = \frac{g_s}{16\pi^2}\, m_s\, \bar{s}_{R\alpha}\, \sigma_{\mu\nu}\, b_{L\beta}\, t^{a\alpha\beta} G^{a\mu\nu}\ . \tag{13}$$

However, these are suppressed by a factor of m_s/m_b and hence generally neglected in the SM analysis. They do give significant contribution in case of SUSY without R-parity under the discussion in this paper though. MSSM contributions are very well studied in the literature. We shall make only brief remarks over here and refer the reader to the literature [10, 11, 12] for a detailed discussion. In MSSM, over and above the usual, W-t loop contributions, one can have charged Higgs-up-squarks, chargino-up-squarks, gluino-down squarks and neutralino down-squarks contributions. Since there is left-right scalar mixing in the squark sector, there is a possibility of a mass-insertion inside the loop (see for instance Fig.2 as example with a mass-insertion inside the loop). Since these are mass-terms of the already decoupled heavy modes, they are included in the corresponding Wilson coefficients that encode the dynamics of heavy modes. So in the MSSM, there are new contributions to the Wilson coefficient of $\mathcal{Q}_7$, the operator basis is usually assumed to be the same as in SM. However, this is not quite true. It has been demonstrated in [29] that there could be 100 extra scalar, vector and tensor-type four quark operators, formally higher order in strong coupling (compared to the SM operators). The 40 vector type operators are generated by two gluino box diagrams and gluino-gluon penguin diagrams. However, the vector four-quark operators do not mix with the SM operators at one-loop and hence contribute only at the next to leading log. The 60 scalar and tensor type operators are generated by the two gluino box diagram. These could in-principle mix with the $\mathcal{Q}_{7,8}$. However, this mixing turns out to be sub-dominant. The scalar and tensor type four-quark operators mix only with the dimension-6 penguins (corresponding to the chirality flip on the external quark) and hence their contribution to the amplitude is suppressed by $m_b/m_{\tilde{g}}$ relative to that of dimension-5 ones [30]. So we shall neglect all this extra 100 operators.

Giving up the restriction of R-parity adds to the list of four quark operators. From an inspection of the super-potential it is straightforward to write down the relevant operators. It is clear that there cannot be any contribution from the λ couplings. One gets 12 new four quark operators from the combinations of two λ'-couplings and 6 new four-quark operators from the combinations of two λ''-couplings. With so many extra operators of different origin, a notation that is intuitively suggestive, compact, unambiguous and at the same time offers convenient expression of summation in formulas is virtually impossible. We make a simple choice for the notation as follows: Keeping the notation for SM operators as a yard-stick, we divide the operators according to their chiralities (the advantage of such a classification would soon become clear). Those operators that lead to $b_{_R} \to s_{_L}$ transition are appended to the list of SM operators whereas the operators leading to $b_{_L} \to s_{_R}$ transition are denoted with a tilde (*i.e.,* in the form $\widetilde{\mathcal{Q}}_i$) and form a new list. Obviously the above two classes of operators are related by $L \to R$ flip. This choice is not without potential ambiguity. For instance, the notation $\mathcal{Q}_9, \mathcal{Q}_{10}$ typically denotes semi-leptonic operators, but since we are not dealing with semi-leptonic process in this paper, there should not be any ambiguity. With these comments we write down the additional operators obtained from RPV.

$\lambda'\lambda'$ case:

$$\mathcal{Q}_{9-11} = (\bar{s}_{L\alpha}\, \gamma^\mu\, b_{L\beta})\ (\bar{q}_{R\beta}\, \gamma_\mu\, q_{R\alpha})\ ;\ q = d, s, b\ , \tag{14}$$

$$\widetilde{\mathcal{Q}}_{9-13} = (\bar{s}_{R\alpha}\, \gamma^\mu\, b_{R\beta})\ (\bar{q}_{L\beta}\, \gamma_\mu\, q_{L\alpha})\ ;\ q = d, s, b, u, c\ , \tag{15}$$

$$\widetilde{\mathcal{Q}}_{3,4} = (\bar{s}_{R\alpha}\, \gamma^\mu b_{R\alpha,\beta}) \sum_{i=u,c,d,s,b} (\bar{q}_{Ri\beta}\, \gamma^\mu\, q_{Ri\beta,\alpha})\ , \tag{16}$$

$$\widetilde{\mathcal{Q}}_{5,6} = (\bar{s}_{R\alpha}\, \gamma^\mu b_{R\alpha,\beta}) \sum_{i=u,c,d,s,b} (\bar{q}_{Li\beta}\, \gamma^\mu\, q_{Li\beta,\alpha})\ . \tag{17}$$

---

[2] For instance see the ref.[3] for an off-shell basis. Ref.[27] gives a careful treatment about the issues regarding equations of motion and effective Lagrangian, often neglected in other works.

[3] The operators are written in such a manner that one does not encounter ill-defined trace of the product of odd number of gamma matrices including a γ_5. This allows them to use the fully anti-commuting γ_5 in dimensional regularization.

$\lambda''\lambda''$ case:

$$\widetilde{\mathcal{Q}}_{1,2} = (\bar{s}_{R\alpha}\,\gamma^{\mu}\,b_{R\alpha,\beta})\;(\bar{c}_{R\beta}\,\gamma_{\mu}\,c_{R\beta,\alpha})\;, \tag{18}$$

$$\widetilde{\mathcal{Q}}_{14,15} = (\bar{s}_{R\alpha}\,\gamma^{\mu}\,b_{R\alpha,\beta})\;(\bar{u}_{R\beta}\,\gamma_{\mu}\,u_{R\beta,\alpha})\;, \tag{19}$$

$$\widetilde{\mathcal{Q}}_{16,17} = (\bar{s}_{R\alpha}\,\gamma^{\mu}\,b_{R\alpha,\beta})\;(\bar{d}_{R\beta}\,\gamma_{\mu}\,d_{R\beta,\alpha})\;. \tag{20}$$

Thus the total number of operators becomes 28 which mix upon QCD renormalization.

C. Wilson Coefficients

The most important operator for the decay $b \to s + \gamma$ is of course the magnetic penguin $\mathcal{Q}_7$. In order to obtain the corresponding C_7 we first need to define the relevant interaction Lagrangian. At this point we would like to emphasize that since we are working in the most general setting of RPV, there is an important distinction in the way we write down the interaction Lagrangian and the Wilson coefficients as compared to ref.[20]. Our analytical formulas contain all possible contributions from RPV including the bilinear RPV couplings. In ref.[20] the treatment of bilinear (RPV) parameters is slightly erroneous. They work in a basis where bilinears (μ_i's) have been rotated away. This *does not* get rid of all the RPV effects beyond those described by the trilinear RPV couplings. RPV mass mixings are still to be found among the fermions and the scalars [13]. In fact such mass mixing effects through the "sneutrino" VEVs, render the definition of the flavor basis of the charged leptons and the down-sector quarks in the formulation of the Lagrangian ambiguous [13]. The problem is totally avoided in our formulation. Our formulae are given in terms of exact mass eigenstates, instead of the often used mass insertion approximation. Because of the RPV mass mixings our formulae for the Wilson coefficients do not factor into the MSSM contributions and RPV contributions as treated in ref.[20]. With these remarks we list here the interaction Lagrangian.

Gluino-quark-squark vertex

$$\mathcal{L}^{\tilde{g}} = g_s\overline{\Psi}(\tilde{g})\Phi^{\dagger}(\tilde{d}_m)\left[\mathcal{G}^{R}_{mi}\frac{1+\gamma_5}{2} + \mathcal{G}^{L}_{mi}\frac{1-\gamma_5}{2}\right]\Psi(d_i) \;+\; \text{h.c.}\;, \tag{21}$$

where,

$$\mathcal{G}^{L^*}_{mi} = -\sqrt{\frac{8}{3}}\,\mathcal{D}^{d}_{im}\;, \qquad\qquad \mathcal{G}^{R^*}_{mi} = \sqrt{\frac{8}{3}}\,\mathcal{D}^{d}_{(i+3)m}\;, \tag{22}$$

with $\mathcal{D}^{d^\dagger}\mathcal{M}^2_{\rm D}\mathcal{D}^{d} = diag\{\mathcal{M}^2_{\rm D}\}$ while $\mathcal{M}^2_{\rm D}$ is 6×6 being the down-squark mass-matrix. Here $i,j,k = 1$ to 3 (same below), $m = 1$ to 6 for the scalar (squark) mass eigenstates.

Chargino(charged-lepton)-quark-squark vertices

$$\mathcal{L}^{\chi^-} = g_2\overline{\Psi}(\chi^-_n)\Phi^{\dagger}(\tilde{u}_m)\left[\mathcal{C}^{L}_{nmi}\frac{1-\gamma_5}{2} + \mathcal{C}^{R}_{nmi}\frac{1+\gamma_5}{2}\right]\Psi(d_i) \;+\text{h.c.}\;, \tag{23}$$

where,

$$\begin{aligned}\mathcal{C}^{L^*}_{nmi} &= -\boldsymbol{V}_{1n}\,\mathcal{D}^{u}_{im} + \frac{y_{u_p}}{g_2}\,V^{pi^*}_{\rm CKM}\,\boldsymbol{V}_{2n}\,\mathcal{D}^{u}_{(p+3)m}\;,\\ \mathcal{C}^{R^*}_{nmi} &= \frac{y_{d_i}}{g_2}\,V^{hi^*}_{\rm CKM}\,\boldsymbol{U}_{2n}\,\mathcal{D}^{u}_{hm} + \frac{\lambda'_{qri}}{g_2}\,V^{hr^*}_{\rm CKM}\,\boldsymbol{U}_{(q+2)n}\,\mathcal{D}^{u}_{hm}\;.\end{aligned} \tag{24}$$

Here, and throughout the paper, the m index counts the scalar mass eigenstates and the n index that of the fermions. Matrix $\mathcal{D}^u$ diagonalizes the 6×6 up-squark mass matrix *i.e.* $\mathcal{D}^{u^\dagger}\mathcal{M}^2_U\mathcal{D}^u = \text{diag}\{\mathcal{M}^2_{\rm U}\}$, and $m = 1$ to 6 for the up-squarks. Similarly $\boldsymbol{V}^\dagger\mathcal{M}_C\boldsymbol{U} = \text{diag}\{\mathcal{M}_{\mathcal{C}}\}$ for the $n = 1$ to 5 charged fermions (charginos and charged leptons).

Neutralino(neutrino)-quark-squark vertices

$$\mathcal{L}^{\chi^0} = g_2\overline{\Psi}(\chi^0_n)\Phi^{\dagger}(\tilde{d}_m)\left[\mathcal{N}^{L}_{nmi}\frac{1-\gamma_5}{2} + \mathcal{N}^{R}_{nmi}\frac{1+\gamma_5}{2}\right]\Psi(d_i) \;+\text{h.c.}\;, \tag{25}$$

where,

$$\mathcal{N}^{L^*}_{nmi} = -\sqrt{2}\,\{\tan\theta_W(\mathcal{Q}_d - T_{3f})\boldsymbol{X}^*_{1n} + T_{3f}\boldsymbol{X}^*_{2n}\}\,\mathcal{D}^d_{im} - \frac{y_{d_i}}{g_2}\boldsymbol{X}^*_{4n}\,\mathcal{D}^d_{(i+3)m} - \frac{\lambda^*_{hip}}{g_2}\boldsymbol{X}^*_{(h+4)n}\mathcal{D}^d_{(p+3)m}\ , \tag{26}$$

$$\mathcal{N}^{R*}_{nmi} = \sqrt{2}\,\tan\theta_W\,\mathcal{Q}_d\,\boldsymbol{X}_{1n}\,\mathcal{D}^d_{(i+3)m} - \frac{y_{d_i}}{g_2}\,\boldsymbol{X}_{4n}\,\mathcal{D}^d_{im} - \frac{\lambda_{hqi}}{g_2}\,\boldsymbol{X}_{(h+4)n}\,\mathcal{D}^d_{qm}\ , \tag{27}$$

where $T_{3f} = -\frac{1}{2}$. The neutral fermions indexed by n have the 7×7 (neutralino-neutrino) mass matrix to be diagonalized by X.

Charged Higgs(slepton)-quark-quark vertices

$$\mathcal{L}^{\phi^-} = g_2\overline{\Psi}(u_n)\Phi^\dagger(\phi^-_m)\left[\widetilde{\mathcal{C}}^L_{nmi}\frac{1-\gamma_5}{2} + \widetilde{\mathcal{C}}^R_{nmi}\frac{1+\gamma_5}{2}\right]\Psi(d_i)\ + \text{h.c.}\ , \tag{28}$$

where,

$$\begin{aligned}\widetilde{\mathcal{C}}^{L^*}_{nmi} &= \frac{y_{u_n}}{g_2}\,V^{ni^*}_{\rm CKM}\,\mathcal{D}^l_{1m}\ ,\\ \widetilde{\mathcal{C}}^{R^*}_{nmi} &= \frac{y_{d_i}}{g_2}\,V^{ni^*}_{\rm CKM}\,\mathcal{D}^l_{2m} + \frac{\lambda_{jki}}{g_2}\,V^{nk^*}_{\rm CKM}\,\mathcal{D}^l_{(j+2)m}\ .\end{aligned} \tag{29}$$

$\mathcal{D}^l$ being the diagonalizing matrix for the 8×8 charged-slepton charged-Higgs mass matrix.

Neutral scalar(sneutrino)-quark-quark vertices

$$\mathcal{L}^{\phi^0} = g_2\overline{\Psi}(d_n)\Phi^\dagger(\phi^0_m)\left[\widetilde{\mathcal{N}}^L_{nmi}\frac{1-\gamma_5}{2} + \widetilde{\mathcal{N}}^R_{nmi}\frac{1+\gamma_5}{2}\right]\Psi(d_i)\ + \text{h.c.}\ , \tag{30}$$

where

$$\begin{aligned}\widetilde{\mathcal{N}}^{L^*}_{nmi} &= -\frac{y_{d_i}}{g_2}\,\delta_{in}\,\frac{1}{\sqrt{2}}\,[\mathcal{D}^s_{2m} - i\,\mathcal{D}^s_{7m}] - \frac{\lambda^*_{pin}}{g_2}\,\frac{1}{\sqrt{2}}\,[\mathcal{D}^s_{(p+2)m} - i\,\mathcal{D}^s_{(p+7)m}]\ ,\\ \widetilde{\mathcal{N}}^{R^*}_{nmi} &= -\frac{y_{d_i}}{g_2}\,\delta_{in}\,\frac{1}{\sqrt{2}}\,[\mathcal{D}^s_{2m} + i\,\mathcal{D}^s_{7m}] - \frac{\lambda_{qni}}{g_2}\,\frac{1}{\sqrt{2}}\,[\mathcal{D}^s_{(q+2)m} + i\,\mathcal{D}^s_{(q+7)m}]\ ,\end{aligned} \tag{31}$$

$\mathcal{D}^s$ being the diagonalizing matrix for the 10×10 neutral scalar mass matrix.

Next we present all the Wilson coefficients at the scale M_W. The most important is of course C_7. It can be decomposed into various contributions as follows.

$$C_7 = C_7^W\ +\ C_7^{\tilde{g}}\ +\ C_7^{\chi^-}\ +\ C_7^{\chi^0}\ +\ C_7^{\phi^-}\ +\ C_7^{\phi^0}\ . \tag{32}$$

The terms from left to right are the SM, gluino, chargino(charged-lepton), neutralino(neutrino), charged scalar(sleptons and Higgs) and neutral scalar(sneutrino) contributions. All except the last one are common to MSSM too. Note, however, that in accordance with the above formulation, we are putting together in $C_7^{\chi^-}$ and $C_7^{\chi^0}$ contributions from the light fermion mass eigenstates, namely the charged leptons and neutrinos. Below we list the individual

contributions for a decay $d_j \to d_i + \gamma$. ($j = 3$ and $i = 2$ for $b \to s + \gamma$) .

$$C_7^W = \frac{3g_2^2}{8}\frac{m_{u_n}^2}{M_W^4}V_{\rm CKM}^{nj}V_{\rm CKM}^{ni*}\left[-F_2\Big(\frac{m_{u_n}^2}{M_W^2}\Big)-\mathcal{Q}_u F_1\Big(\frac{m_{u_n}^2}{M_W^2}\Big)\right] , \tag{33}$$

$$C_7^{\tilde g} = \frac{2g_s^2}{3}\,\frac{\mathcal{Q}_{\tilde d}}{M_{\tilde d_m}^2}\left[\mathcal{G}^{R}_{mj}\mathcal{G}^{L^*}_{mi}\,\frac{M_{\tilde g}}{m_{d_j}}\,F_4\Big(\frac{M_{\tilde g}^2}{M_{\tilde d_m}^2}\Big) + \mathcal{G}^{L}_{mj}\mathcal{G}^{L^*}_{mi}F_2\Big(\frac{M_{\tilde g}^2}{M_{\tilde d_m}^2}\Big)\right] , \tag{34}$$

$$C_7^{\chi^-} = \frac{\mathcal{C}^{R}_{nmj}\mathcal{C}^{L^*}_{nmi}}{4M_{\tilde u_m}^2}\left[\frac{M_{\chi_n^-}}{m_{d_j}}\mathcal{Q}_{\tilde u}F_4\Big(\frac{M_{\chi_n^-}^2}{M_{\tilde u_m}^2}\Big)+F_3\Big(\frac{M_{\chi_n^-}^2}{M_{\tilde u_m}^2}\Big)\right]+\frac{\mathcal{C}^{L}_{nmj}\mathcal{C}^{L^*}_{nmi}}{4M_{\tilde u_m}^2}\left[\mathcal{Q}_{\tilde u}\,F_2\Big(\frac{M_{\chi_n^-}^2}{m_{\tilde u_m}^2}\Big)+F_1\Big(\frac{M_{\chi_n^-}^2}{M_{\tilde u_m}^2}\Big)\right] , \tag{35}$$

$$C_7^{\chi^0} = \frac{1}{4}\,\frac{\mathcal{Q}_{\tilde d}}{M_{\tilde d_m}^2}\left[\mathcal{N}^{R}_{nmj}\mathcal{N}^{L^*}_{nmi}\,\frac{M_{\chi_n^0}}{m_{d_j}}\,F_4\Big(\frac{M_{\chi_n^0}^2}{M_{\tilde d_m}^2}\Big) + \mathcal{N}^{L}_{nmj}\mathcal{N}^{L^*}_{nmi}\,F_2\Big(\frac{M_{\chi_n^0}^2}{M_{\tilde d_m}^2}\Big)\right] , \tag{36}$$

$$\begin{aligned} C_7^{\phi^-} &= \frac{1}{M_{\tilde\ell_m}^2}\,\widetilde{\mathcal{C}}^{R}_{nmj}\widetilde{\mathcal{C}}^{L^*}_{nmi}\,\frac{m_{u_n}}{m_{d_j}}\,\left[(\mathcal{Q}_d-\mathcal{Q}_u)\,F_4\Big(\frac{m_{u_n}^2}{M_{\tilde\ell_m}^2}\Big)-\mathcal{Q}_u\,F_3\Big(\frac{m_{u_n}^2}{M_{\tilde\ell_m}^2}\Big)\right] \\ &\quad+\frac{1}{M_{\tilde\ell_m}^2}\,\widetilde{\mathcal{C}}^{L}_{nmj}\widetilde{\mathcal{C}}^{L^*}_{nmi}\,\left[(\mathcal{Q}_d-\mathcal{Q}_u)\,F_2\Big(\frac{m_{u_n}^2}{M_{\tilde\ell_m}^2}\Big)-\mathcal{Q}_u\,F_1\Big(\frac{m_{u_n}^2}{M_{\tilde\ell_m}^2}\Big)\right] , \end{aligned} \tag{37}$$

$$C_7^{\phi^0} = \frac{-\mathcal{Q}_d}{M_{S_m}^2}\left[\widetilde{\mathcal{N}}^{R}_{nmj}\widetilde{\mathcal{N}}^{L^*}_{nmi}\,\frac{m_{d_n}}{m_{d_j}}\,F_3\Big(\frac{m_{d_n}^2}{M_{S_m}^2}\Big) + \widetilde{\mathcal{N}}^{L}_{nmj}\widetilde{\mathcal{N}}^{L^*}_{nmi}\,F_1\Big(\frac{m_{d_n}^2}{M_{S_m}^2}\Big)\right] . \tag{38}$$

Each term includes, implicitly, summation over the n fermion and m scalar mass eigenstates, except that the unphysical Goldstone modes are not to be included. The latter contributions are incorporated into the gauge invariant C_7^W result. Contributions to $\widetilde{C}_7$ except for the case of C_7^W are obtained by replacement $L \leftrightarrow R$. The C_7^W term above is given in terms of explicit couplings, rather than the effective coupling vertices. In accordance with the notation of other terms, the vertices involved in the C_7^W term above should be two 'L'-couplings the 'R' counterparts of which vanish. Any term above of the LL type, *i.e.* with two 'L'-couplings has, like C_7^W term, a chirality flip from the b-quark external line. The rest of the terms, of the RL type, have chirality flip inside the loop as illustrated also by the explicit fermion mass ratio factor. Contributions from terms of RR type to C_7 coefficient needs chirality flip from the s-quark external line and are neglected here, as also in most of the literature. One can similarly map out the details for the chirality structure for the $\widetilde{C}_7$ coefficient. We note, however, that the latter receives extra contributions from yet another class of diagrams with λ''_{ijk}-couplings and the chirality flip on the b-quark. Such contributions are missing in the coefficient C_7, except for the ones suppressed with the chirality flip from the s-quark.

$$\begin{aligned} \widetilde{C}_7^{\lambda''} &= \frac{1}{4M_{\tilde u_m}^2}\lambda^{''*}_{hnj}\lambda''_{kni}\mathcal{D}^{u*}_{h+3,m}\mathcal{D}^{u}_{k+3,m}\left[-\mathcal{Q}_d F_1\left(\frac{m_{d_n}^2}{M_{\tilde u_m}^2}\right)+\mathcal{Q}_{\tilde u}F_2\left(\frac{m_{d_n}^2}{M_{\tilde u_m}^2}\right)\right] \\ &\quad+\frac{1}{4M_{\tilde d_m}^2}\lambda^{''*}_{nhj}\lambda''_{nki}\mathcal{D}^{d*}_{h+3,m}\mathcal{D}^{d}_{k+3,m}\left[-\mathcal{Q}_u F_1\left(\frac{m_{u_n}^2}{M_{\tilde d_m}^2}\right)+\mathcal{Q}_{\tilde d}F_2\left(\frac{m_{u_n}^2}{M_{\tilde d_m}^2}\right)\right] . \end{aligned} \tag{39}$$

Similarly one can obtain the expressions for the C_8 and $\widetilde{C}_8$ by introducing the colour factors at the relevant places. The loop-functions F_{1-4} are the Inami-Lim functions, given as:

$$F_1(x) = \frac{1}{12\,(1-x)^4}\,(2+3\,x-6\,x^2+x^3+6\,x\,\ln x) , \tag{40}$$

$$F_2(x) = \frac{1}{12\,(1-x)^4}\,(1-6\,x+3\,x^2+2\,x^3-6\,x^2\,\ln x) , \tag{41}$$

$$F_3(x) = \frac{1}{2(1-x)^3}\,(-3+4\,x-x^2-2\,\ln x) , \tag{42}$$

$$F_4(x) = \frac{1}{2(1-x)^3}\,(1-x^2+2\,x\,\ln x) . \tag{43}$$

Below we write down the non-zero effective Wilson coefficients for the current-current operators.

$$C_2 = -\frac{G_F}{\sqrt{2}} V^{cs*}_{\rm CKM} V^{cb}_{\rm CKM} \ , \tag{44}$$

$$C_9 = -\frac{1}{8M^2_{\tilde{s}_m}} \lambda'_{i31} \lambda'^*_{j21} \mathcal{P}^s \ , \tag{45}$$

$$C_{10} = -\frac{1}{8M^2_{\tilde{s}_m}} \lambda'_{i32} \left[\lambda'^*_{j22} \mathcal{P}^s + y_s \mathcal{P}^{s'} \right] \ , \tag{46}$$

$$C_{11} = -\frac{1}{8M^2_{\tilde{s}_m}} \lambda'^*_{j23} \left[\lambda'_{i33} \mathcal{P}^s + y_b \mathcal{P}^{s'} \right] \ , \tag{47}$$

$$\widetilde{C}_1 = -\frac{1}{8m^2_{\tilde{d}_m}} \lambda''_{2i2} \lambda^{''*}_{2j3} \mathcal{D}^d_{3+j,m} \mathcal{D}^{d*}_{3+i,m} = -\widetilde{C}_2 \ , \tag{48}$$

$$\widetilde{C}_9 = -\frac{1}{8M^2_{\tilde{s}_m}} \lambda'_{i12} \lambda'^*_{j13} \mathcal{P}^s \ , \tag{49}$$

$$\widetilde{C}_{10} = -\frac{1}{8M^2_{\tilde{s}_m}} \lambda'^*_{j23} \left[\lambda'_{i22} \mathcal{P}^s + y_s \mathcal{P}^{s'} \right] \ , \tag{50}$$

$$\widetilde{C}_{11} = -\frac{1}{8M^2_{\tilde{s}_m}} \lambda'_{i32} \left[\lambda'^*_{j33} \mathcal{P}^s + y_b \mathcal{P}^{s'} \right] \ , \tag{51}$$

$$\begin{aligned} \widetilde{C}_{12} &= \frac{-1}{8M^2_{\tilde{\ell}_m}} \lambda'_{i12} \lambda'^*_{j13} \mathcal{D}^l_{2+i,m} \mathcal{D}^{l*}_{2+j,m} \ , \\ &\quad - \frac{1}{8M^2_{\tilde{\ell}_m}} y_s y_b \mathcal{D}^l_{2,m} \mathcal{D}^{l*}_{2,m} V^{us*}_{\rm CKM} V^{ub}_{\rm CKM} \\ &\quad - \frac{1}{8M^2_{\tilde{\ell}_m}} \lambda'^*_{j13} V^{us}_{\rm CKM} y_s \mathcal{D}^l_{2+i,m} \mathcal{D}^{l*}_{2,m} \ , \end{aligned} \tag{52}$$

$$\begin{aligned} \widetilde{C}_{13} &= -\frac{1}{8M^2_{\tilde{\ell}_m}} \lambda'_{i22} \lambda'^*_{j23} \mathcal{D}^l_{2+i,m} \mathcal{D}^{l*}_{2+j,m} \\ &\quad - \frac{1}{8M^2_{\tilde{\ell}_m}} y_s y_b \mathcal{D}^l_{2,m} \mathcal{D}^{l*}_{2,m} V^{cs*}_{\rm CKM} V^{cb}_{\rm CKM} \\ &\quad - \frac{1}{8M^2_{\tilde{\ell}_m}} \lambda'^*_{j23} V^{cs}_{\rm CKM} y_s \mathcal{D}^l_{2+i,m} \mathcal{D}^{l*}_{2,m} \ , \end{aligned} \tag{53}$$

$$\widetilde{C}_{14} = -\frac{1}{8m^2_{\tilde{d}_m}} \lambda''_{1i2} \lambda^{''*}_{1j3} \mathcal{D}^d_{3+j,m} \mathcal{D}^{d\dagger}_{3+i,m} = -\widetilde{C}_{15} \ , \tag{54}$$

$$\widetilde{C}_{16} = -\frac{1}{8m^2_{\tilde{u}_m}} \lambda''_{i12} \lambda^{''*}_{j13} \mathcal{D}^u_{3+j,m} \mathcal{D}^{u\dagger}_{3+i,m} = -\widetilde{C}_{17} \ , \tag{55}$$

where,

$$\mathcal{P}^s = \frac{1}{2} \left(\mathcal{D}^s_{2+i,m} + i \mathcal{D}^s_{7+i,m} \right) \left(\mathcal{D}^s_{2+j,m} + i \mathcal{D}^s_{7+j,m} \right)^* \ , \tag{56}$$

$$\mathcal{P}^{s'} = \frac{1}{2} \left(\mathcal{D}^s_{2+i,m} + i \mathcal{D}^s_{7+i,m} \right) \left(\mathcal{D}^s_{2,m} + i \mathcal{D}^s_{7,m} \right)^* \ . \tag{57}$$

Here, y_s and y_b denote the strange and the bottom Yukawas. Again the sum over repeated indices is assumed and the unphysical Goldstone modes are to be dropped from the sum. Note that the terms proportional to Yukawas are missing in the ref [20]. This could lead to interesting contributions with the λ' on one vertex and a SM Yukawa on the other vertex with a RPV mass mixing effect hidden within the $\mathcal{P}^{s'}$ expression. In the language of mass-insertion approximation, these kind of contributions involve a RPV mass-insertion (*e.g.* from a μ_i or a B_i coupling) along the scalar propagator.

IV. THE ANOMALOUS DIMENSION MATRIX AND RG RUNNING

The RG evolution from the scale M_W to the scale appropriate for the decay dynamics (m_b) is described by eq.(6). This requires the knowledge of the anomalous dimension matrix γ_{ij} (ADM). Derivation of γ_{ij} presents many subtleties and was a main obstacle in the consistent calculation of the decay rate about a decade ago [2, 3]. Below we mention the salient features of the calculation.

- Since QCD does not know the sign of γ_5 there is no mixing among the sets of $\widetilde{\mathcal{Q}}_i$ and $\mathcal{Q}_i$ operators. Thus the full basis of 28 operators splits into two invariant sub-spaces of 11 and 17 operators related by $L \leftrightarrow R$ inter-change.
- An operator of a dimensionality n can mix into the operators of dimensionality $\leq n$. Thus the current-current four quark operators influence the RG evolution of (chromo)magnetic Wilson coefficients, but not the other way around.
- At the one-loop level current-current operators do not mix with the (chromo)magnetic penguins. Thus, one has to evaluate this mixing at the two loop-level while still working at the leading log approximation. Because of this, the ADM and hence the Wilson coefficients at the LL are found to be regularization scheme-dependent. Such a scheme-dependence cancels with the corresponding scheme-dependence of the possible finite one-loop (but $O(\alpha_s^0)$) contributions from certain four-quark operators to the matrix elements of $b \to s+\gamma$. Such contributions vanish in any four dimensional as well as t-Hooft-Veltman regularization scheme but not in naive dimensional regularization. Such a situation is taken care of by expressing the ADM and the Wilson coefficients in a scheme independent manner [31].
- Since one needs to perform a two-loop calculation, one must properly take into account the contributions from the so called evanescent operators (that vanish in the limit $D = 4$ dimension) while working in the $D \neq 4$ dimension.

With these remarks in mind one can formally write down the decay amplitude as:

$$A = C_7 \langle\, s\gamma \,|\mathcal{Q}_7|\, b\rangle_{tree} + \widetilde{C}_7\ \langle s\gamma\,|\widetilde{\mathcal{Q}}_7|\, b\rangle_{tree} + \sum_{i=1}^{11} C_i \langle\, s\gamma\,|\mathcal{Q}_i|\, b\rangle_{1-loop} + \sum_{i=1}^{17} \widetilde{C}_i \langle\, s\gamma\,|\widetilde{\mathcal{Q}}_i|\, b\rangle_{1-loop}\ . \tag{58}$$

In order to obtain a decay rate that is regularization scheme-independent, we must express the decay amplitude A in terms of scheme-independent effective coefficients. Decay amplitude A is written as:

$$A = C_7^{\rm eff}\ \langle\, s\gamma\,|\mathcal{Q}_7|\, b\rangle_{tree}\ +\ \widetilde{C}_7^{\rm eff}\ \langle s\gamma\,|\widetilde{\mathcal{Q}}_7|\, b\rangle_{tree}\ . \tag{59}$$

To derive the effective coefficients one makes the observation that in whatever scheme one chooses to work, the one-loop matrix elements of the current-current operators for the decay $b \to s + \gamma$ is always proportional to the tree-level matrix elements of the (chromo)magnetic operators. Thus, one can write

$$\begin{aligned}
< s\gamma|\mathcal{Q}_i|b >_{1-\rm loop} &= y_i < s\gamma|\mathcal{Q}_7|b >_{\rm tree}, \\
< s\,{\rm gluon}|\mathcal{Q}_i|b >_{1-\rm loop} &= z_i < s\,{\rm gluon}|\mathcal{Q}_8|b >_{\rm tree}\ , &(60)\\
< s\gamma|\widetilde{\mathcal{Q}}_i|b >_{1-\rm loop} &= \widetilde{y}_i < s\gamma|\widetilde{\mathcal{Q}}_7|b >_{\rm tree}\ , &(61)\\
< s\,{\rm gluon}|\widetilde{\mathcal{Q}}_i|b >_{1-\rm loop} &= \widetilde{z}_i < s\,{\rm gluon}|\widetilde{\mathcal{Q}}_8|b >_{\rm tree}\ . &(62)
\end{aligned}$$

In order to find out the proportionality factors y_i, z_i etc., one has to evaluate the finite contribution due to the insertion of certain four-quark operators into the diagrams with a closed b quark loop (in the NDR scheme). The only operators that could give finite contribution are the ones with the chirality structure (LL)(RR) or (RR)(LL). Within SM basis, these are $\mathcal{Q}_5, \mathcal{Q}_6$. With RPV you could also have $\widetilde{\mathcal{Q}}_5, \widetilde{\mathcal{Q}}_6$ and $\mathcal{Q}_{11}, \widetilde{\mathcal{Q}}_{11}$. The results for $\{y_i\}$, $\{z_i\}$, $\{\widetilde{y}_i\}$ and $\{\widetilde{z}_i\}$ are given as:

$$y_i \ = \ \begin{cases} -\frac{1}{3} & i = \mathcal{Q}_5 \\ -1 & i = \mathcal{Q}_6,\ \mathcal{Q}_{11} \\ 0 & \text{otherwise} \end{cases} \qquad z_i \ = \ \begin{cases} 1 & i = \mathcal{Q}_5 \\ 0 & \text{otherwise} \end{cases}$$

$$\widetilde{y}_i \ = \ \begin{cases} -\frac{1}{3} & i = \widetilde{\mathcal{Q}}_5 \\ -1 & i = \widetilde{\mathcal{Q}}_{11},\ \widetilde{\mathcal{Q}}_6 \\ 0 & \text{otherwise} \end{cases} \qquad \widetilde{z}_i \ = \ \begin{cases} 1 & i = \widetilde{\mathcal{Q}}_5 \\ 0 & \text{otherwise} \end{cases} \tag{63}$$

With this one can write down the scheme-independent Wilson coefficients as:

$$\begin{aligned}
C_7^{\rm eff}(\mu) &= C_7(\mu) + \sum_{i=1}^{11} y_i\, C_i(\mu)\,, \\
C_8^{\rm eff}(\mu) &= C_8(\mu) + \sum_{i=1}^{11} z_i\, C_i(\mu)\,, \\
\widetilde{C}_7^{\rm eff}(\mu) &= \widetilde{C}_7(\mu) + \sum_{i=1}^{17} \widetilde{y}_i\, \widetilde{C}_i(\mu)\,, \\
\widetilde{C}_8^{\rm eff}(\mu) &= \widetilde{C}_8(\mu) + \sum_{i=1}^{17} \widetilde{z}_i\, \widetilde{C}_i(\mu)\,, \\
C_{\mathcal{Q}_i,\widetilde{\mathcal{Q}}_i}^{\rm eff}(\mu) &= C_{\mathcal{Q}_i,\widetilde{\mathcal{Q}}_i}(\mu)\,.
\end{aligned} \tag{64}$$

The index i above runs over only the current-current operators.

The RG evolution of the effective coefficients is determined by the scheme-independent effective ADM. The RG equations are given as:

$$\frac{d}{\ln\mu} C_k^{\rm eff}(\mu) = \frac{\alpha_s}{4\pi} \gamma_{jk}^{\rm eff}\; C_j^{\rm eff}(\mu)\,. \tag{65}$$

Here $C_k^{\rm eff}$ are the components of a column vector $\vec{C}^{\rm eff}$ which contains coefficients $C_k^{\rm eff}$ as well as $\widetilde{C}_k^{\rm eff}$. Since QCD does not know the sign of γ_5, these two sets of coefficients do not mix. The effective ADM at leading log is obtained as:

$$\hat{\gamma}^{(0)\rm eff} = \begin{pmatrix} \gamma_L^{\rm eff} & 0 \\ 0 & \gamma_R^{\rm eff} \end{pmatrix}\,. \tag{66}$$

$\gamma_L^{\rm eff}$ represents QCD mixing of 11 operators whose chirality structure is similar to those of SM operators. $\gamma_R^{\rm eff}$ represents the mixing of 17 operators whose chirality structure is obtained by $L \leftrightarrow R$ replacement with SM like operators. We present the explicit matrices in the appendix A.

In general, the solution of the RGE for the Wilson-coefficients is given by

$$\vec{C}^{\rm eff}(\mu) = V \left[\left(\frac{\alpha_s(M_W)}{\alpha_s(\mu)} \right)^{\vec{\gamma}_D^{\rm eff}/2\beta_0} \right]_D V^{-1}\; \vec{C}^{\rm eff}(M_W)\,, \tag{67}$$

where V diagonalizes $(\gamma^{\rm eff})^T$

$$\gamma_D^{\rm eff} = V^{-1} (\gamma^{\rm eff})^T V\,. \tag{68}$$

$\beta_0 = 23/3$ is the one-loop beta-function and $\vec{\gamma}_D^{\rm eff}$ is the vector containing the eigenvalues of $\gamma^{\rm eff}$. In our case

$$\begin{aligned}
\vec{\gamma}_D^{\rm eff} = (&-16 \quad -16 \quad -16 \quad -16 \quad -16 \quad -16 \quad -16 \\
&-16 \quad -8 \quad -8 \quad -8 \quad -8 \quad 4 \quad 4 \\
&4 \quad 4 \quad \tfrac{28}{3} \quad \tfrac{28}{3} \quad \tfrac{32}{3} \quad \tfrac{32}{3} \quad 2.233 \\
&2.233 \quad 6.266 \quad 6.266 \quad -13.791 \quad -13.791 \quad -6.486 \quad -6.486)\,.
\end{aligned} \tag{69}$$

With $\alpha_s(M_Z) = 0.121$ and $\mu = m_b = 4.2$ GeV, the coefficients $C_7^{\rm eff}(m_b)$ and $\widetilde{C}_7^{\rm eff}(m_b)$ are given as:

$$\begin{aligned}
C_7^{\rm eff}(m_b) &= -0.351\, C_2^{\rm eff}(M_W) + 0.665\, C_7^{\rm eff}(M_W) + 0.093\, C_8^{\rm eff}(M_W) - 0.198\, C_9^{\rm eff}(M_W) \\
&\quad -0.198\, C_{10}^{\rm eff}(M_W) - 0.178\, C_{11}^{\rm eff}(M_W)\,,
\end{aligned}$$

$$\begin{aligned}
\widetilde{C}_7^{\rm eff}(m_b) &= 0.381\, \widetilde{C}_1^{\rm eff}(M_W) + 0.665\, \widetilde{C}_7^{\rm eff}(M_W) + 0.093\, \widetilde{C}_8^{\rm eff}(M_W) - 0.198\, \widetilde{C}_9^{\rm eff}(M_W) \\
&\quad -0.198\, \widetilde{C}_{10}^{\rm eff}(M_W) - 0.178\, \widetilde{C}_{11}^{\rm eff}(M_W) + 0.510\, \widetilde{C}_{12}^{\rm eff}(M_W) + 0.510\, \widetilde{C}_{13}^{\rm eff}(M_W) \\
&\quad +0.381\, \widetilde{C}_{14}^{\rm eff}(M_W) - 0.213\, \widetilde{C}_{16}^{\rm eff}(M_W)\,.
\end{aligned} \tag{70}$$

The numbers multiplying the different Wilson coefficients are all of the same size, hence no term can be neglected *a priori*.

Finally, the branching fraction for $Br(b \to s+\gamma)$ is expressed through the semi-leptonic decay $b \to u|ce\bar{\nu}$ so that the large bottom mass dependence ($\sim m_b^5$) and uncertainties in CKM elements cancel out.

$$Br(b \to s+\gamma) = \frac{\Gamma(b \to s+\gamma)}{\Gamma(b \to u|c\,e\,\bar{\nu}_e)} Br_{\rm exp}(b \to u|c\,e\,\bar{\nu}_e) \; , \tag{71}$$

where $Br_{\rm exp}(b \to u|c\,e\,\bar{\nu}_e) = 10.5\%$. Here the presence of RPV couplings offers new decay channels and new contributions to the semi-leptonic decay rate. In principle, lepton flavor violating couplings demand a summation over the three (anti)neutrino mass eigenstates (assuming the neutralinos are heavy) before squaring the amplitude. In considering the λ'-coupling contributions, the dominating neutrino mass terms would be at one-loop level. As all the neutrino states have close to zero masses, and very small admissible mixings with the gauginos and the Higgsinos, we neglect these effects here and stick to effective massless electroweak neutrinos. The summation is then taken simply over the three families. Under the same spirit, we neglect here the effects from the lepton flavor violating couplings that could change the electroweak character of physical electron. The partial widths in the expression above are given, at the LL order with m_u^2/m_b^2 set to zero, as

$$\begin{aligned}
\Gamma(b \to s\gamma) &= \frac{\alpha m_b^5}{64\pi^4}(|C_7^{\rm eff}(\mu_b)|^2 + |\widetilde{C}_7^{\rm eff}(\mu_b)|^2) \; , \\
\Gamma(b \to u|c\,e\,\bar{\nu}) &= \frac{m_b^5}{192\pi^3}\frac{1}{32}\left\{f(\epsilon)\left[|2A + C_2|^2 + B_2\right] + \; |B_1|^2 + |C_1|^2\right\} \; , \\
f(\epsilon) &= 1 - 8\epsilon^2 + 8\epsilon^6 - \epsilon^8 - 24\epsilon^4 \log\epsilon \; , \\
A &= 2\sqrt{2} G_F V_{\rm CKM}^{ts} \; , \\
B_r &= \sum_{i=1}^{3} \frac{1}{M_{\tilde{\ell}_l}^2}\left[\lambda_{ij1}\lambda'^{*}_{mn3} D^{l*}_{2+m,l} D^{l}_{2+j,l}\right] V_{\rm CKM}^{rn} \; + \; \left[h_e \lambda'^{*}_{mn3} D^{l*}_{2+m,l} D^{l}_{2,l}\right] V_{\rm CKM}^{rn} \quad r = 1,2 \; , \\
C_r &= -\sum_{i=1}^{3} \frac{\lambda'_{i3k}\lambda'^{*}_{1mn}}{M_{\tilde{d}_l}^2} D^{d*}_{3+k,l} D^{d}_{3+n,l} V_{\rm CKM}^{rm} \; .
\end{aligned}$$

Here $\epsilon = m_c/m_b$. The above expression for the semi-leptonic decay rate is the most general one that also includes the contribution from bilinear-trilinear combination of R-parity violating parameters (the term $\propto h_e$) which has been generally missed in the earlier studies. Such contributions have been shown to play a very important role as elaborated in detail in our parallel report on $b \to s+\gamma$ [24] and for the case of quark dipole moments in [23].

V. NUMERICAL RESULTS ON THE TRILINEAR COUPLINGS

Our presentation of the numerical results in this paper restricts to the effects of the combinations of trilinear couplings only. We present some details of the numerical results on the phenomenologically interesting λ'-couplings. The λ''-couplings are found not to give interesting results — a feature we will comment on at the end of the section. To set the stage for the more detailed discussion on our numerical results, we first recall the salient features of this particular decay within the MSSM. Within MSSM, the story is already quite complicated. In the limit of exact SUSY there is no contribution to the decay rate due to the cancellations among particles and sparticles [32]. With SUSY broken, there could be gluino, chargino, charged Higgs and neutralino contributions depending on what particle is exchanged in the loop. Chirality flip can be induced by mass-insertion on the internal or the external fermion line. The squark mass matrices are not necessarily flavor diagonal and the flavor violation is introduced as family off-diagonal mass insertion in the loop. The couplings of quarks and squarks to the neutral gauge bosons and gauginos are flavor diagonal. The more exact treatment, as adopted here, is to use the mass eigenstates for the particles running in the loop and hence have the flavor violation effects absorbed into the effective couplings which contain the corresponding elements of the squark diagonalizing matrices. With the inclusion of RPV couplings, there are a lot more flavor violating couplings, and more new types of admissible diagrams. These are described in our mass eigenstate expressions most naturally by simply enriching the effective couplings.

The significance of the MSSM contribution to the decay rate is highly dependent on the choice of values for the background parameters of the model. Over and above the delicate issue of cancellations among various contributions, it is also a function of 'how much' and 'where' does one introduces the flavor violation. The approaches in the literature can be broadly classified into two categories. (a) The so called constrained MSSM (cMSSM) where one

starts with the universal boundary conditions at the high scale and derives the weak-scale spectrum by RG evolution. CKM angles are then the sole source of flavor violation[33]. In such a scenario, the dominant contributions are due to the chargino and charged Higgs loops. Gluino and neutralino couplings being flavor diagonal, rely on flavor violating mass mixing terms in the down squark mass matrix generated from RG evolution. Such mixings within cMSSM are typically very small to contribute to the decay rate. Gluino contributions suffer from hard GIM cancellations. While neutralino contributions can escape GIM cancellations through Yukawa couplings but cannot compete with chargino contribution that are enhanced by heavy top in the loop[11]. (b) Another end of the spectrum is simply the unconstrained scenario. Here, the idea is to assume arbitrary structure for the squark mass matrices and derive the weak-scale bounds on the off-diagonal flavor violating entries by requiring to reproduce the decay rate within the experimental uncertainties [34]. We adopt the philosophy of unconstrained scenario studies. However, we will switch-off the R-parity conserving flavor violations, except that from the CKM matrix to focus on the effect of the RPV parts. In fact, we will focus on a pair of λ'-couplings (or λ''-couplings) at a time while the other flavor violating parameters that are otherwise not theoretically constrained will be switched off. Note that the flavor violations originating from λ'-couplings are essentially of supersymmetric origin though SUSY breaking, and phenomenologically viable, scalar and gaugino masses are needed to avoid the intrinsic SUSY cancellations.

Before our analysis of RPV contributions, we have first checked our code for the case of MSSM in order to reproduce the trends and features obtained in the previous works. Here, the matching can be done at a qualitative level only. Most of the detailed numerical results in the literature for the case of MSSM are worked out within the cMSSM scenario. The low energy spectrum obtained by RG evolution and a particular SUSY breaking boundary condition contains correlations among various parameters and there are RG induced flavor violations mixed with that from the CKM matrix. With this limitations, our code does reproduce qualitatively, trends and features of various contributions obtained by others [10, 11, 12]. We give an illustration of our MSSM results in Figs.3,4 and 5. For a scenario characterized by squarks around 300 GeV, sleptons around 150 GeV, down-type Higgs and A parameter 300 GeV, (up-type Higgs mass and B_0 parameter determined from potential minimization condition), gaugino $M_2 = 200$ GeV (assuming the relationship $M_1 = 0.5M_2, M_3 = 3.5M_2$) and $\mu = -300$ GeV for Fig.3 and 300 GeV for Fig.5 (note that the MSSM parameter μ is denoted by μ_0 in our model notation), we plot branching fraction versus tanβ. As is well known, the charged Higgs contribution is of the same sign as the SM whereas the sign of chargino contribution depends on the sign of the product $A_t\mu$ (see Fig. 4 where we have plotted various contributions to the Wilson coefficients). In the large tanβ region, the decay rate is completely dictated by the chargino contributions and hence the enhancement or the suppression of the rate actually depends on whether $A_t\mu$ is positive or negative, respectively. Within the framework of mSUGRA (see ref.[12]), choosing the gaugino masses to be positive, forces A_t to be negative at the weak scale, and hence one requires a positive μ for the rate at large tanβ to fall within the experimental limits. In Fig.3,5 we plot the decay rate for negative and positive μ respectively with A_t fixed to be positive. One can see in the figures that the decay rate does fall initially with tanβ and then rises in case of negative μ but for positive μ, due to constructive interference between chargino and charged-Higgs the rate rises with tanβ. This can be easily compared with the Fig.2 of ref.[12], for example.

While investigating the influence of RPV we kept the spectrum similar to the one selected for the case of MSSM with sign of μ negative and tan$\beta = 37$. Note that in the large tanβ region QCD corrections drastically suppress the rate at the scale m_b (see for instance Fig.3). This is expected because, in the large tanβ region, the Wilson coefficient C_7 is negative due to large negative chargino contribution and at the scale m_b after the QCD correction there is a destructive interference between C_2 and C_7. The choice of spectrum is guided by requiring that in the MSSM limit we do obtain branching fraction well within experimental limits. Now the purpose is to investigate the behaviour of branching fraction once we turn on the knob of R-parity violation. As we will see, both, enhancement as well as suppression is possible depending on which operator(s) are playing the major role. Both, the direct contribution, through the magnetic penguin, and the effect induced by QCD renormalization, through the various four-quark operators are significant.

Due to the large number of RPV parameters (48 just from the superpotential, with more from the soft SUSY breaking sector), without further knowledge of their plausible range of values it is impossible to extract any useful information on a phenomenological study, with all of them playing a role at the same time. Hence, the sensible thing to do at this stage is to focus on a minimal number at a time and study their possible impact. For the case at hand, a pair of parameters is taken at a time, while all the others are switched off. We discuss first the λ'-couplings. There are two possible combinations in which two non-zero λ' can give a finite contribution. These are (A) $\lambda'_{i3j}\lambda'^{*}_{h2k}$ and (B) $\lambda'^{*}_{ij3}\lambda'_{hk2}$. We illustrate their effects in more detail below.

We will compare below the probable bounds we obtained with the similar bounds on the relevant combination of λ'-couplings in the literature. We have, first, to bring to the readers attention that the existing bounds in the literature are typically obtained assuming a sparticle spectrum of around 100 GeV. However, such a low lying spectrum is very

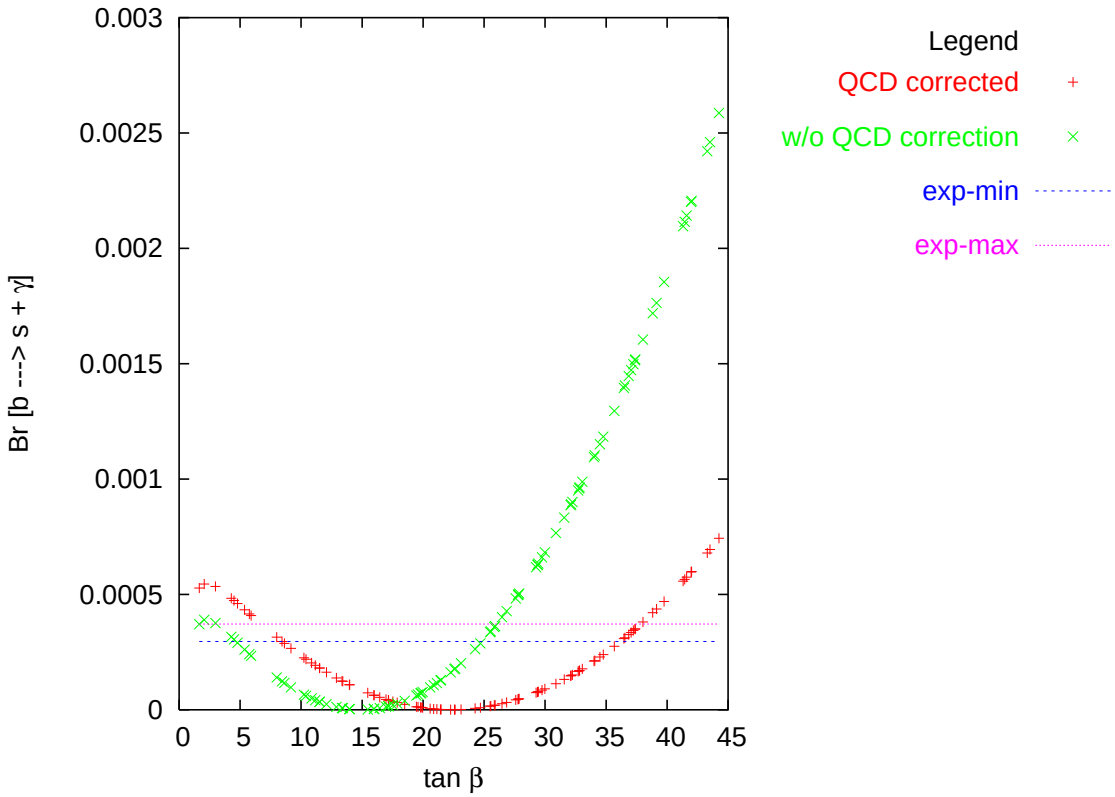

FIG. 3: Branching ratio as a function of tanβ in MSSM with A_t positive and μ negative. The '+' sign is for the QCD corrected rate and the '×' sign for the rate without QCD corrections. Two horizontal lines in this Fig. and all the following figures for branching fraction is the experimental uncertainty at 1σ. See text for the values of various parameters.

dangerous for $b \to s + \gamma$ [4] and quite unrealistic at least for the squarks. In consideration of that, and for a better comparison with the available $b \to s + \gamma$ result for the R-conserving contributions (of the MSSM), we stick to a slightly heavier spectrum of 300 GeV squarks. Hence, the existing bounds must be rescaled by a factor of three for a better comparison with our bounds. Moreover, for some the combinations that contribute to $b \to s + \gamma$ there do not exist any direct bound. We have then made use of the best bounds available on the individual parameters to obtain a bound on such a combination.

1. *Case A:* $\lambda'_{i3j}\lambda'^{*}_{h2k}$

If the indices i, j, h, k are un-constrained, one can form 81 combinations of two λ'-couplings that can in principle contribute. However, in the limit there is no flavor off-diagonal mixing in the (s)neutrino mass matrix, the combination with $i \neq h$ will not contribute. The case $j \neq k$ requires extra source of flavor off-diagonal squark mixing to contribute; hence is also not of interest here. So we shall confine ourselves to the case $i = h$ and $j = k$ and hence study the impact of only nine (9) combinations, picking one of them to be non-zero at a given time. Note that so long as one sticks to the phenomenologically required suppression in all the flavor off-diagonal mass mixings from SUSY, the RPV contributions which require such mixings would be doubly suppressed and hence highly unlikely to be of any numerical significance. For the magnetic penguin operators, the contribution is of LL type.

The above combination will lead to a $b_R \to s_L$ transition with m_b mass-insertion on external line. The contribution

[4] To be exact, the top squarks contribute directly through the chargino diagram without the CKM suppression and have to be heavier. The bottom and strange squarks contribute, if their flavor violating mixings are nonzero. They are hence likely to be required to be heavier too. Otherwise, we can actually live with only heavier stops but a light sparticle here. Such a split in sparticle spectrum is considered unlikely as it goes in the opposite direction as predictions from most available SUSY breaking models.

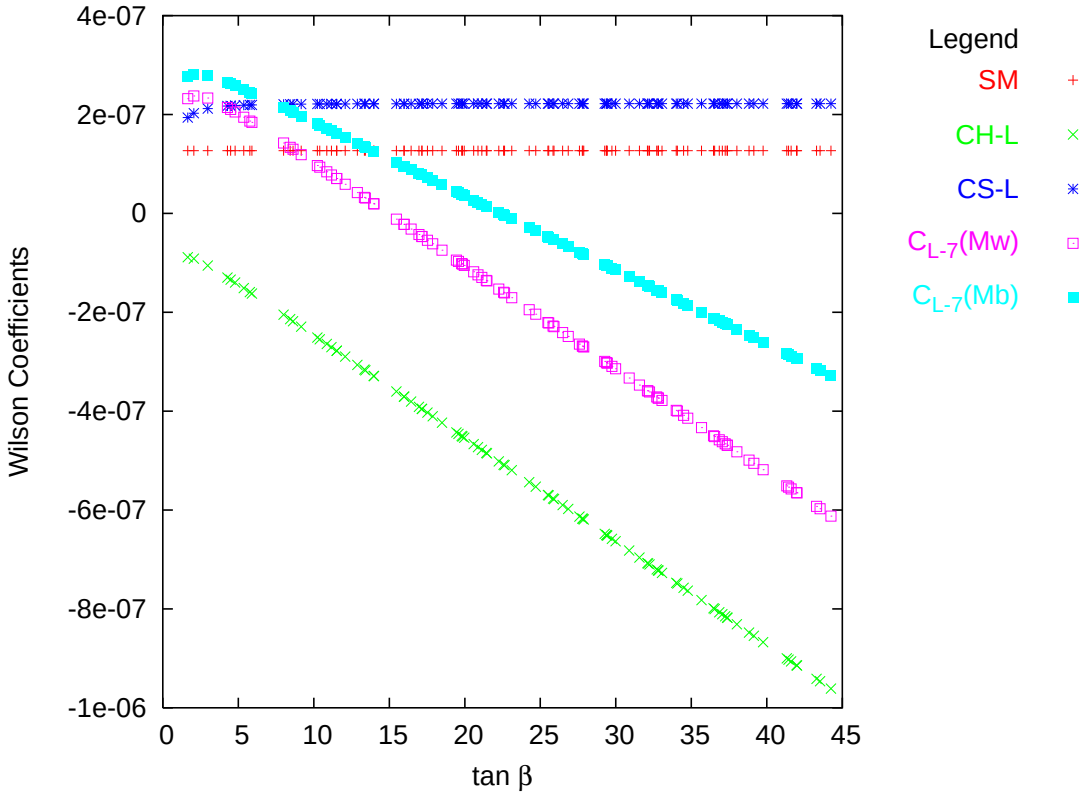

FIG. 4: Various contributions to Wilson coefficients versus tanβ. SM (line with symbol '+') and charged Higgs (denoted as CS-L, line with '*' sign) are of the same sign (positive) whereas the chargino contribution (denoted as CH-L, line with 'x' sign) has a strong tanβ dependence and is of opposite sign (negative) because $A_t\mu < 0$.

can come from chromo(magnetic) penguins (only sneutrino and neutrino loops are possible) or from the current-current operators $\mathcal{Q}_{9,10,11}$. Sneutrino loops being proportional to the inverse of light slepton mass, are dominant compared to the neutrino loops which are suppressed by heavier squark mass. The important feature here is that the RPV contributions interfere with the SM and the MSSM contributions. Of the possible nine combinations, we will discuss three representative combinations with best bounds. The other six combinations follow similar pattern, as their contributions have a similar structure.

In our numerical analysis, we take real and equal values for two λ'-couplings at a time. As discussed above and illustrated by the analytical formulae, the contributions depend on the complex product. The strategy here then simplifies the results to one-parameter scenario for easy presentation, without compromising the physics. Consider the influence of the combinations $|\lambda'_{13k}\lambda'_{12k}|$. For $k = 1, 2$ the physics is identical because the relevant Wilson coefficients ($C_{9,10}$) have identical structure and so we shall discuss the combination $|\lambda'_{132}\lambda'_{122}|$. In Fig.6 we have plotted the branching ratio against λ'_{132} ($= \lambda'_{122}$). Interestingly, the rate falls below the experimental limit (at $\lambda'_{132} = \lambda'_{122} = 0.07$) with increasing λ' value, reaches a minimum and then rises again (the rise is not shown in the fig.). To understand this behavior we have plotted all the relevant Wilson coefficients against λ' values in Fig.7. It can be clearly seen that $C_7(M_W)$ is falling with increasing λ' value. This is because of destructive interference between the negative R-parity conserving contribution (sum of W-boson, charged Higgs and Chargino loop) and the positive sneutrino loop contribution, as seen in the figure. At the scale m_b after QCD running there is again destructive interference between the dominant tree level contribution from C_{10} and C_7 [see eq. (70)], because of which $C_7(m_b)$ further falls with increasing λ' value. So because of these destructive interference, the branching ratio is falling below the experimental limit and we obtain a bound of $|\lambda'_{132}\lambda'_{122}| < 4.9 \times 10^{-3}$, to be compared with a rescaled existing bound of 3×10^{-2}. In Fig.8, we have plotted the branching ratio against λ'_{333} ($= \lambda'_{323}$). Unlike the above case, here the relevant current-current Wilson coefficient C_{11} has a more important role to play. Not only does the scheme-independent effective coefficient $C_{11}^{\rm eff}$ influence $C_7(m_b)$ through RG running, it also contributes to $C_7^{\rm eff}$ directly. The effect cancels with the R-parity conserving contributions and hence $C_7^{\rm eff}(M_W)$ is seen to reduce with increasing λ' value. Even at the scale m_b, after QCD running there is a destructive interference between the R-parity conserving and R-parity violating parts and hence $C_7^{\rm eff}$ at m_b further reduces resulting in the branching fraction that falls with the

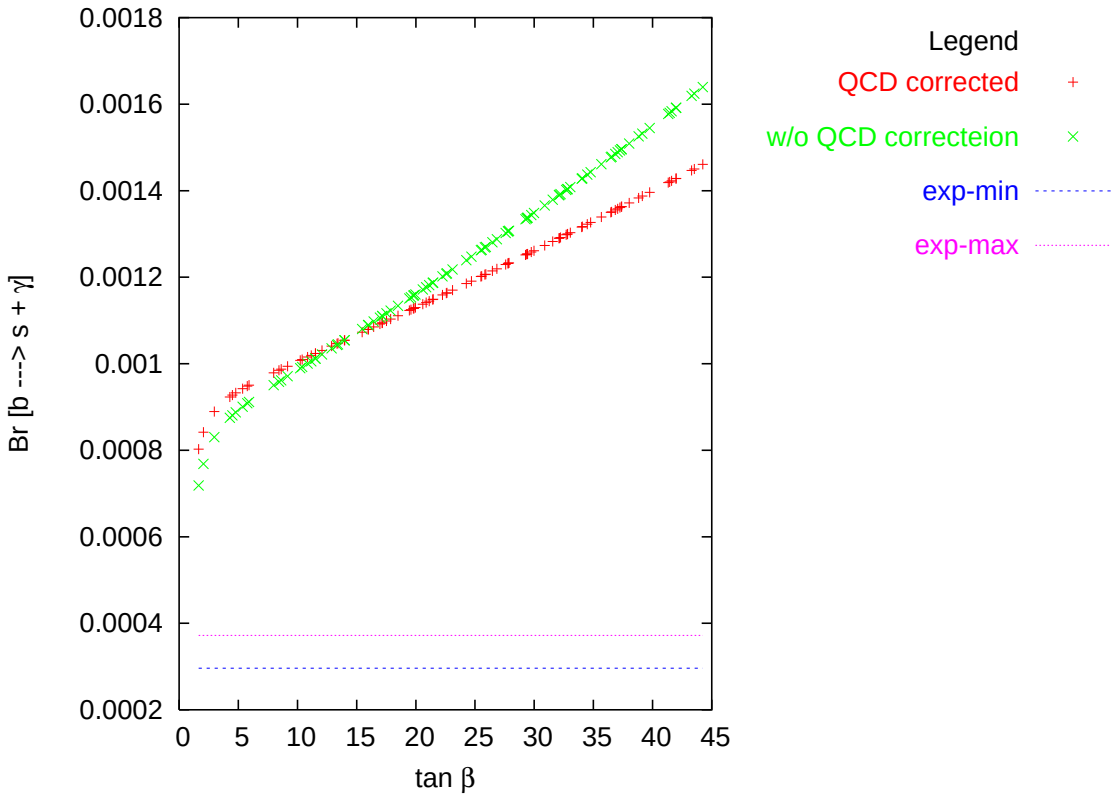

FIG. 5: Same as Fig.3, but with sign of μ positive.

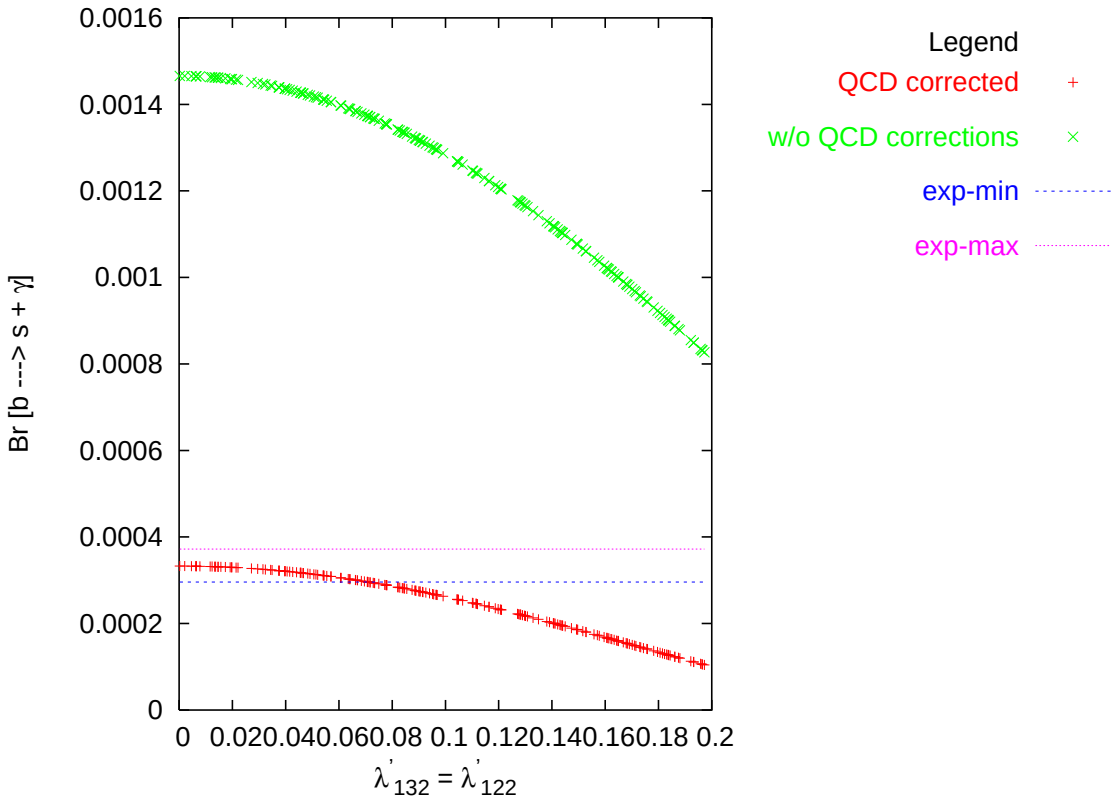

FIG. 6: Branching fraction as a function of λ'_{132} ($= \lambda'_{122}$).

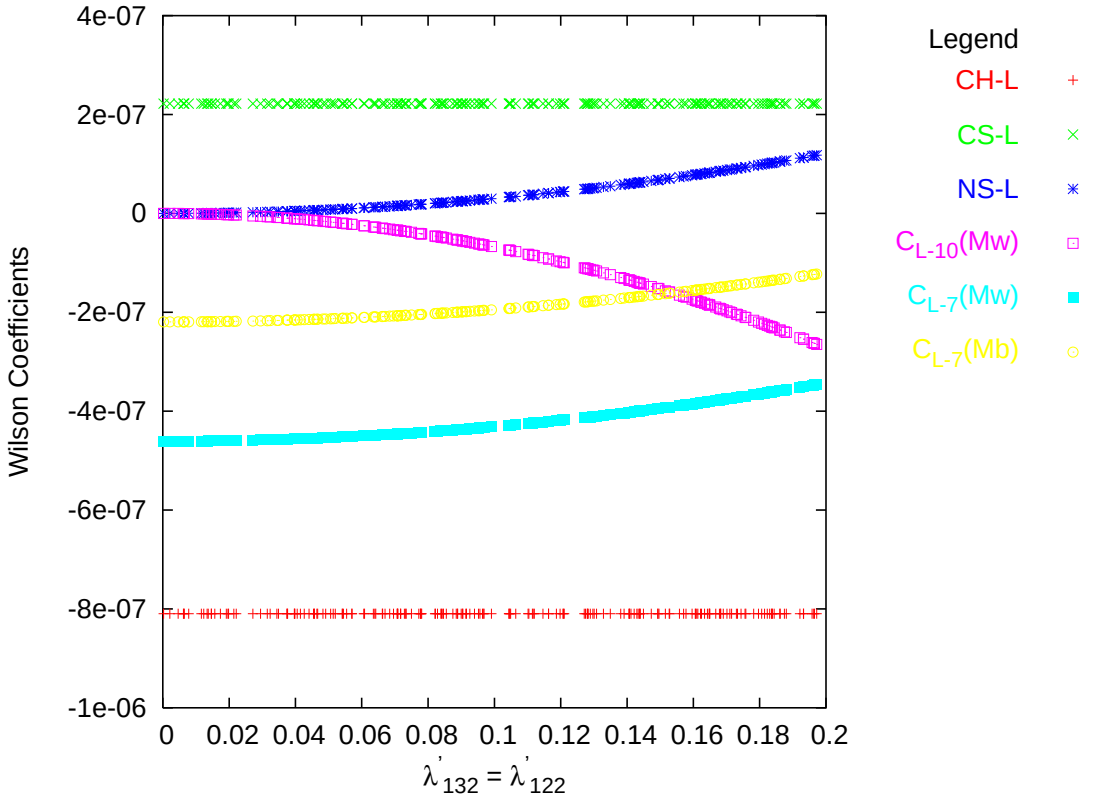

FIG. 7: Wilson coefficients as a function of λ'_{132} $(= \lambda'_{122})$. CH,CS,NS stand for the chargino, charged-Higgs and sneutrino contributions, respectively. The letter 'L' indicates that these contributions go into C_7. Similar notation would apply to the following figures. The letter 'R'(L) would indicate that the contribution goes into coefficients with(without) tilde.

RPV coupling. The fall is much stronger compared to the previous case. We obtain a bound of $|\lambda'_{333}\lambda'_{323}| < 1.6 \times 10^{-3}$ to be compared with the rescaled existing bound of $(1-3) \times 10^{-2}$ [35].

2. *Case B:* $\lambda'^{*}_{ij3}\lambda'_{hk2}$

Such a combination leads to a $b_L \to s_R$ transition for m_b mass insertion on the external line. This would mean that the b and s quark at the effective vertices would be right handed. It contributes to the Wilson coefficients of several operators. These include the $\widetilde{C}_{7,8}$ coefficients of the (chromo)magnetic penguins, via charged lepton, charged slepton, neutrino and sneutrino loop. Interestingly, in the SM and MSSM, this coefficient does not receive much contribution. The above combination can also contribute to Wilson coefficients of the current-current operators, $\widetilde{\mathcal{Q}}_9$ to $\widetilde{\mathcal{Q}}_{13}$. These current-current contributions are mostly the dominant ones but not always as we will soon see.

As discussed at length in case (A), we must require $i = h$ and $j = k$ and hence case (B) then effectively consists of the combinations $\lambda'^{*}_{ij3}\lambda'_{ij2}$. Consider Fig.10 where we have plotted the branching fraction against non-vanishing λ'_{233} $(= \lambda'_{232})$. We get a bound $|\lambda'_{233}\lambda'_{232}| < 1.9 \times 10^{-2}$, to be compared with the rescaled existing bound of 4.4×10^{-1} [35]. The mild behaviour of branching fraction suggests the existence of cancellations. In Fig.11 we have plotted branching fraction against λ'_{113} $(= \lambda'_{112})$ and obtain a bound of $|\lambda'_{113}\lambda'_{112}| < 1.4 \times 10^{-2}$. Although the branching fraction behaves more or less similarly in both the above cases, the underlying dynamics is quite different. To better appreciate the differences, we have plotted the relevant Wilson coefficients in Fig.12 for the combination $|\lambda'_{233}\lambda'_{232}|$ and in Fig.13 for the combination $|\lambda'_{113}\lambda'_{112}|$. In Fig.12, the horizontal line (circles) is the large R-parity conserving contribution to $C_7(m_b)$ which does not interfere with the RPV contributions going into $\widetilde{C}_7$. The surprising feature is the large (though less than R-parity conserving contribution) positive contribution of $\widetilde{C}_7(M_W)$. This is surprising because it receives dominant negative sign contribution from the charged-slepton (crosses in the figure) whereas the positive sign sneutrino contribution (star marks in figure) is sub-dominant. Here again, the requirement of scheme-independence plays an important role because $\widetilde{C}_7^{\rm eff}(\mu) = \widetilde{C}_7(\mu) - \widetilde{C}_{11}(\mu)$. It is the large negative sign contribution

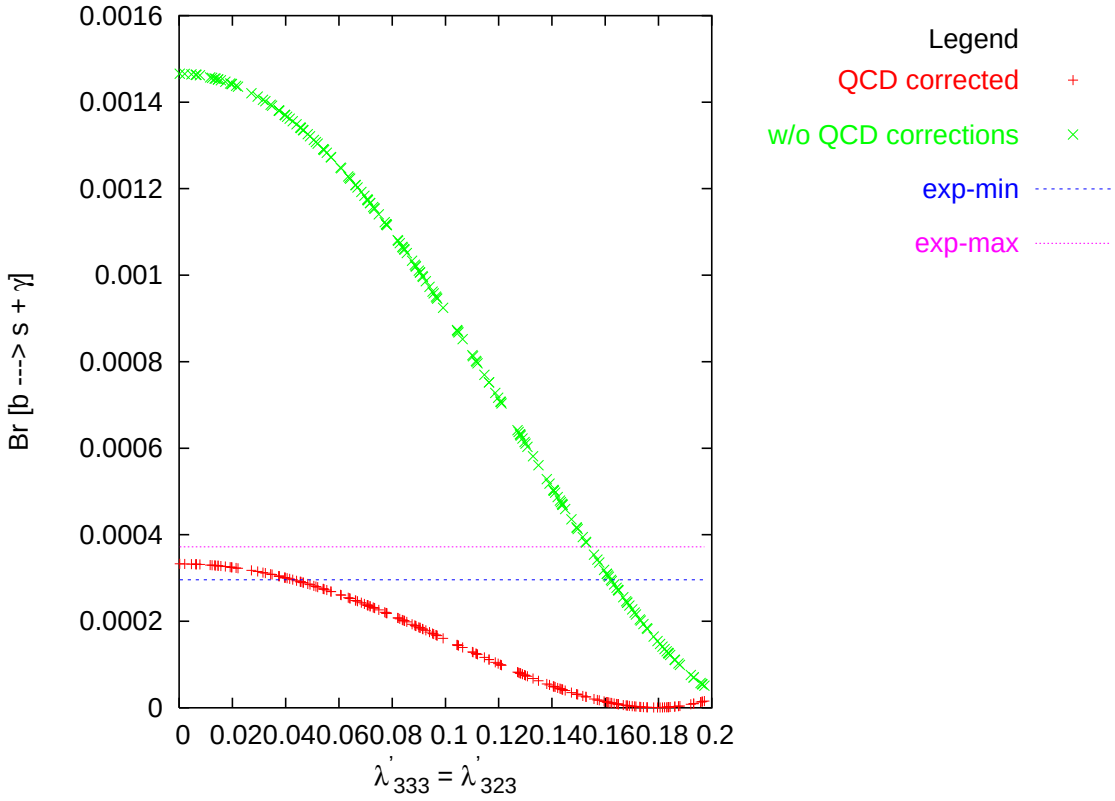

FIG. 8: Branching fraction as a function of λ'_{333} ($= \lambda'_{323}$).

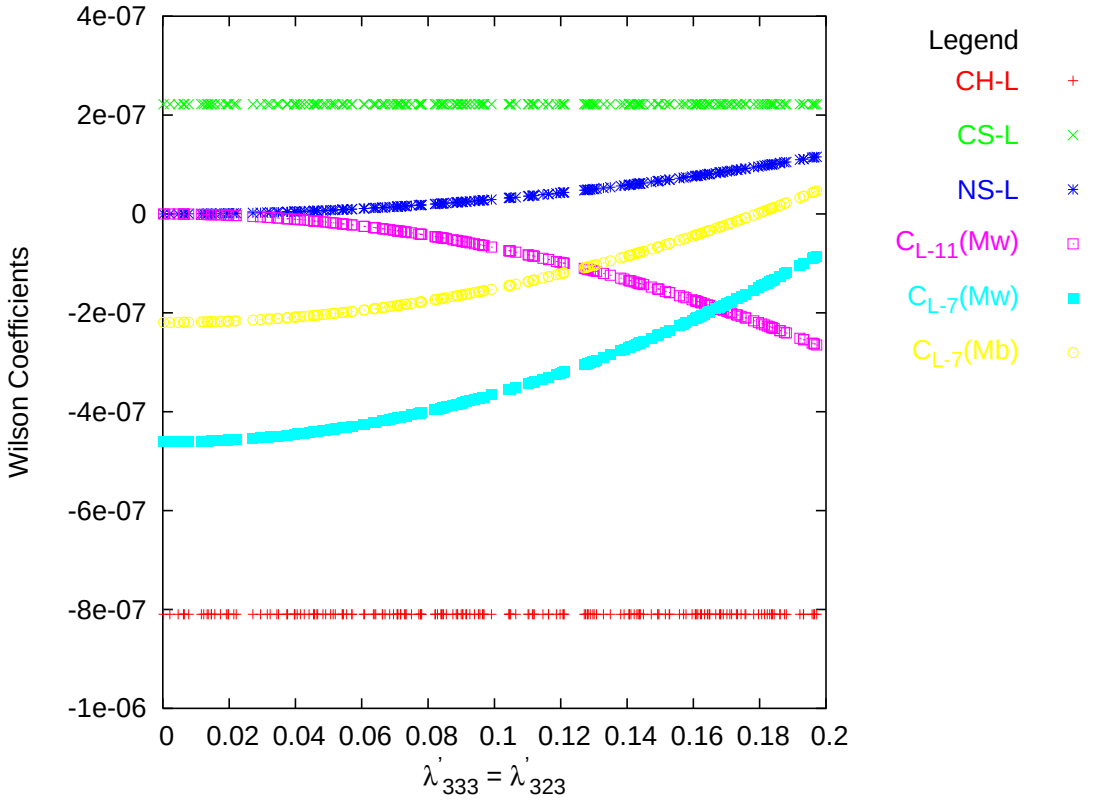

FIG. 9: Relevant Wilson coefficients as a function of λ'_{333} ($= \lambda'_{323}$).

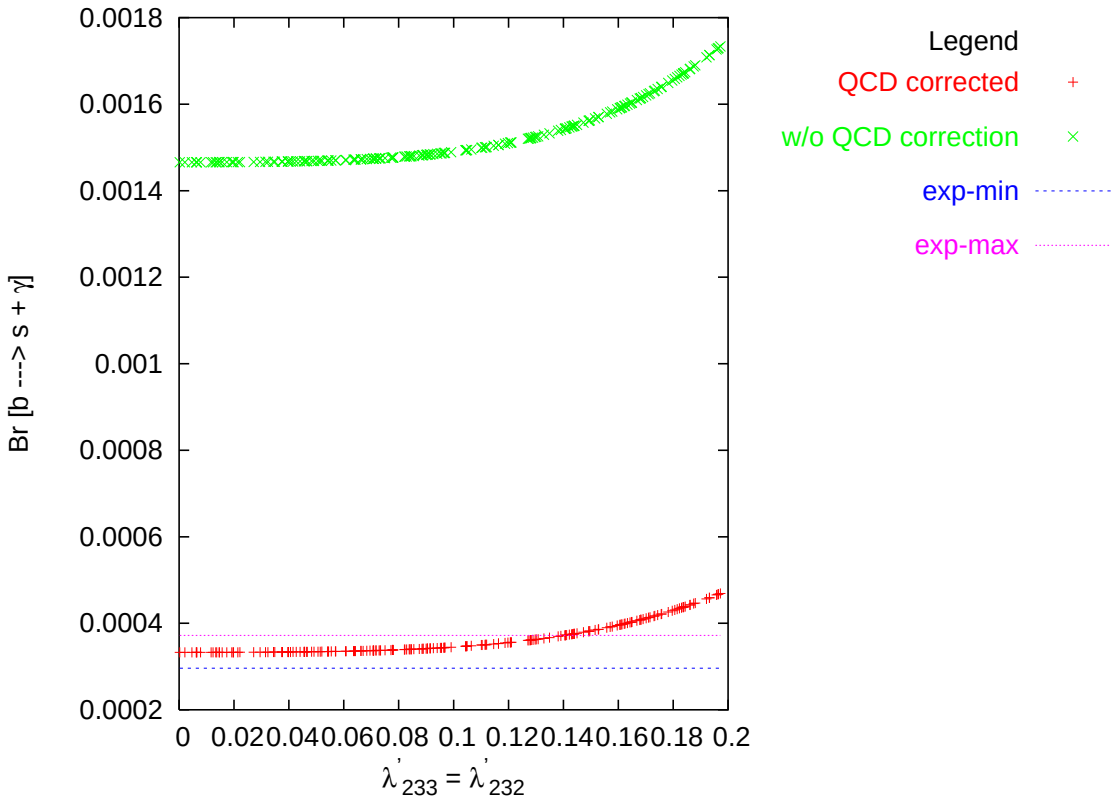

FIG. 10: Branching ratio as a function of λ'_{233} ($= \lambda'_{232}$).

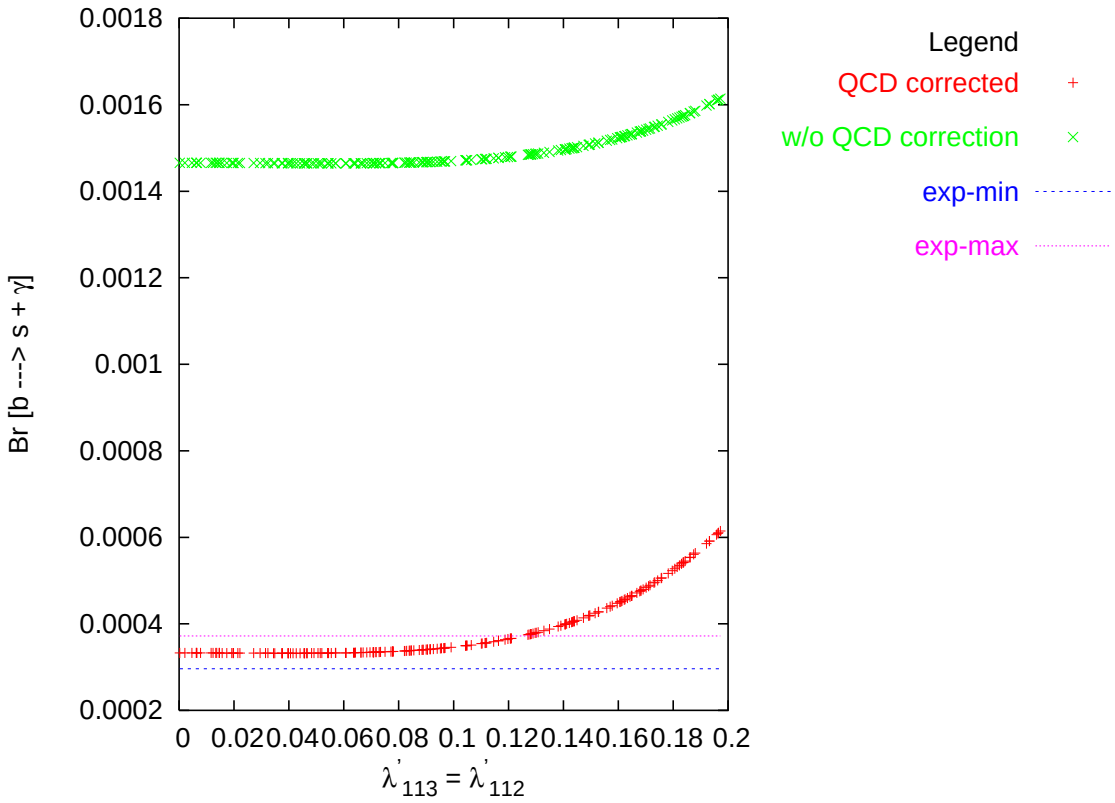

FIG. 11: Branching ratio as a function of λ'_{113} ($= \lambda'_{112}$).

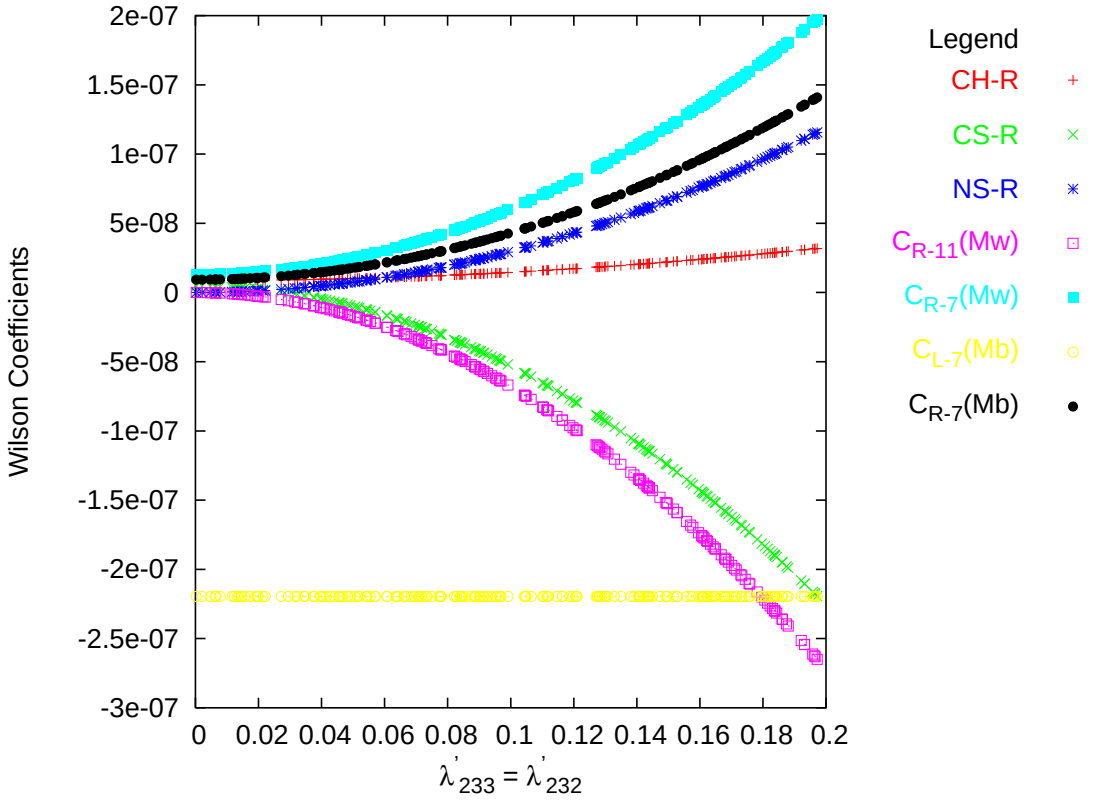

FIG. 12: Relevant Wilson coefficients as a function of λ'_{233} ($= \lambda'_{232}$).

from $\widetilde{C}_{11}(M_W)$ which adds up with the positive sneutrino contribution and dictates the behaviour of $\widetilde{C}_7(M_W)$. At the scale m_b after QCD running, there is some suppression in the Wilson coefficient. Consider the case of the combination $|\lambda'_{113}\lambda'_{112}|$ (see Fig.13). It has a peculiarity of the charged-scalar loop contribution slightly dominating the contribution from current-current Wilson coefficient $\widetilde{C}_9$. This suggests that it is not always true that tree-level contribution dominates. Such a dominance can be traced to two effects : (a) In contrast to the tree level contribution, a charged slepton loop contribution has contributions from two diagrams corresponding to photon being emitted from a charged slepton ($\propto$ to loop function F_2) and the photon being emitted from an up-type quark ($\propto F_1$). (b) The values of loop functions depend on the mass of the quark in the loop – the lighter the quark less the suppression. Thus, provided that there is no CKM suppression, up-quark-charged-slepton loop dominates over the top-quark-charged-slepton loop and in fact can also dominate over the tree level contribution. That there is no CKM suppression in both the above cases can be easily verified from the formulae of the Wilson coefficients. Also the uniform dominance of charged slepton loop over sneutrino loop can be accounted for by the argument (a) above. Since there are two possible diagrams for charged slepton loop it brings in a charge factor of $(2/3 + 1 = 5/3)$ which is five times bigger than the charge factor coming from the down-squark in the sneutrino loop. However, the charged-slepton and sneutrino loop contributions always come with opposite sign and hence there are cancellations.

In TableI, we have listed bounds that we have obtained for the various λ'-coupling combinations among the cases (A) and (B). As far as one restricts oneself to the situation of two non-zero trilinear λ'-couplings, case (A) and case (B) are the only combinations that can contribute. With non-zero bilinears as well, or additional non-zero trilinears, there could be more combinations that can contribute. For instance one can have a combination of $\lambda'_{i3j}\lambda'_{hk2}$, giving rise to a neutrino or a neutral scalar loop for the penguins. Since the overall process conserves lepton number, the above combination obviously needs to be supplemented with two more L-violating couplings. This could be from a Majorana mass-insertions for neutrino or sneutrino in the loop. However, such a contribution would be further suppressed and hence we skip presenting explicit results of the kind.

In all the above discussion, we have assumed that all the couplings are real and positive. It would be interesting to consider the possibility when there is a relative phase resulting in a relative negative sign among the chosen non-vanishing pair of λ' couplings. It turns out that such a case does not affect the bounds much. For the case (B) with dominant contributions from RPV couplings, it obviously cannot affect the decay rate which is modulus squared of Wilson coefficient. However for case (A), a negative or a positive sign can lead to constructive or destructive

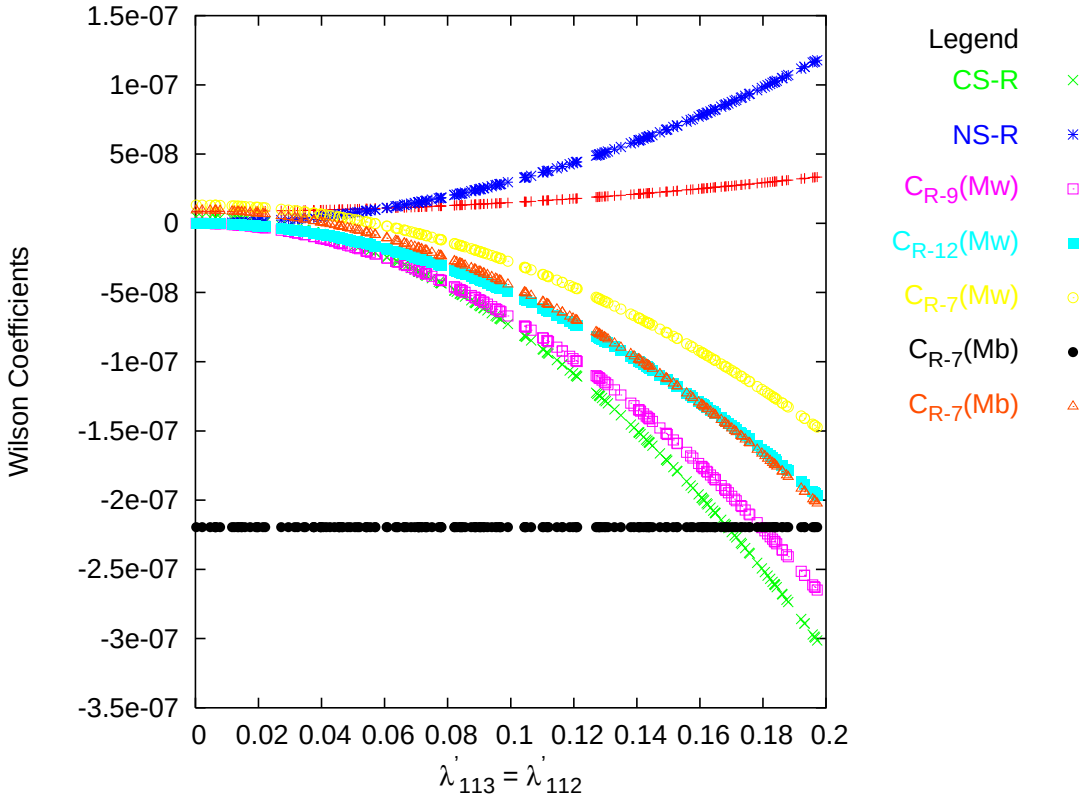

FIG. 13: Relevant Wilson coefficients as a function of λ'_{113} $(= \lambda'_{112})$.

TABLE I: Bounds on the various products of λ' obtained compared with the appropriately rescaled existing bounds [35]

Product $\lvert\lambda'\lambda'\rvert$	**Our bound**	**Existing bound**	**Wilson coeff.**
Case A			
131.121	4.9×10^{-3}	2×10^{-3}	C_7, C_9
132.122	4.9×10^{-3}	3×10^{-2}	C_7, C_{10}
133.123	1.6×10^{-3}	7.2×10^{-5}	C_7, C_{11}
231.221	4.9×10^{-3}	2×10^{-2}	C_7, C_9
232.222	4.9×10^{-3}	2×10^{-2}	C_7, C_{10}
233.223	1.6×10^{-3}	2×10^{-2}	C_7, C_{11}
331.321	4.9×10^{-3}	$(1-3) \times 10^{-2}$	C_7, C_9
332.322	4.9×10^{-3}	$(1-3) \times 10^{-2}$	C_7, C_{10}
333.323	1.6×10^{-3}	$(1-3) \times 10^{-2}$	C_7, C_{11}
Case B			
113.112	1.4×10^{-2}	1.3×10^{-3}	$\widetilde{C}_7, \widetilde{C}_9$
123.122	1.4×10^{-2}	1.3×10^{-3}	$\widetilde{C}_7, \widetilde{C}_{10}$
133.132	1.9×10^{-2}	7.2×10^{-5}	$\widetilde{C}_7, \widetilde{C}_{11}$
213.212	1.4×10^{-2}	1.3×10^{-3}	$\widetilde{C}_7, \widetilde{C}_9$
223.222	1.4×10^{-2}	1.3×10^{-3}	$\widetilde{C}_7, \widetilde{C}_{10}$
233.232	1.9×10^{-2}	4.4×10^{-1}	$\widetilde{C}_7, \widetilde{C}_{11}$
313.312	1.4×10^{-2}	1.3×10^{-3}	$\widetilde{C}_7, \widetilde{C}_9$
323.322	1.4×10^{-2}	1.3×10^{-3}	$\widetilde{C}_7, \widetilde{C}_{10}$
333.332	1.9×10^{-2}	$(1.3-9.2) \times 10^{-1}$	$\widetilde{C}_7, \widetilde{C}_{11}$

interference between R-parity conserving and violating contributions. A relative negative sign though changes the sign of the slope for the branching fraction it does not alter its magnitude. Thus, the only implication as compared to the earlier bound which (for instance) was due to a branching fraction rising above the experimental limit, would now change to a bound due to the branching fraction falling below the experimental limit. The change in the magnitude of the bound is however nominal.

Finally, we comment briefly on contributions from λ''-couplings. We obtain no useful bounds on the λ''-couplings. The main reason behind this is that squark spectrum of 300 GeV is heavy enough to suppress the λ'' contributions. However, a lighter spectrum (although not viable due to large MSSM contributions) cannot lead to enhancement because of certain cancellations taking place. This provides a nice example of the interesting role played by the QCD running and hence worth a brief discussion. The combinations responsible for contributing to the decay rate can be written as: $\lambda''^{*}_{hn3}\lambda''_{kn2}$ from the up-squark loop and $\lambda''^{*}_{nh3}\lambda''_{nk2}$ from the down squark loop, thus contributing to $\widetilde{C}_{7,8}$. Depending on the particular value for the indices, there could also be contributions from the current-current operators with Wilson coefficients, $\widetilde{C}_1(=-\widetilde{C}_2), \widetilde{C}_{14}(=-\widetilde{C}_{15}), \widetilde{C}_{16}(=-\widetilde{C}_{17})$. It might appear that the relative negative signs for the above coefficients leads to cancellations and hence there is no impact on the decay rate. This is not what is happening. There are cancellations, but these result rather from the form of $\widetilde{C}_7$ at the scale (m_b) (see eq.(70). Taking into account, the antisymmetry in the last two indices, one can form 18 combinations from the above mentioned general form of the λ'' contributions (12 combinations contributing to the down-squark loop and 9 to the up-squark loop but 3 three combinations common to both). There are two reasons that kill the contributions. In a few cases, the loop level contribution is accompanied by current-current Wilson coefficients pairs $\widetilde{C}_{14}$ and $\widetilde{C}_{16}$, or $\widetilde{C}_1$ and $\widetilde{C}_{16}$. Although these pairs contribute about equal magnitude with identical sign, at the scale m_b after QCD running these are multiplied by about equal coefficients but with opposite sign and hence the cancellations. The rest of the combinations get contributions from only one among the above pairs and hence cannot suffer from above cancellations. In this case, they all require flavor violating mass-insertions for (s)particles in the loop. The only exception to above two cases is the combination $\lambda''^{*}_{313}\lambda''_{212}$ for which we get a bound of 0.5. This bound is very weak when compared to existing bound from other sources(6.2×10^{-3}[35]).

VI. CONCLUSION

In summary, we present a complete analysis of the decay rate $b\to s+\gamma$ at the leading log order for the generic supersymmetric SM, or SUSY without R-parity. Unlike previous studies on the topic, our results are fully generic, admitting all possible forms of R-parity violation without *a priori* assumption. We use exact mass eigenstates in our formulae, hence free from the otherwise commonly used mass-insertion approximation. In case one prefers, our formulation does provide perturbative approximations through which the explicit dependence on all RPV parameters can be extracted [13]. We consider the analytical results useful for any detailed study on the model in relation to the radiative B decay.

In the numerical implementation of the analytical formulas our focus, is on the λ' couplings. For simplicity and feasibility, we keep two non-vanishing λ'-couplings. The choice of the mass spectrum and various parameters of the model is dictated by the requirement that in the limit of R-parity conserving SUSY, the branching ratio falls within the experimental limits. Then, switching on the non-zero values of the (combination of two) λ'-couplings allows us to trace their contribution and obtain bounds on the class of RPV parameters from imposing the experimental constraints. In this aspect, the strategy is common to many of the earlier studies. We find that RPV contributions not only expand the relevant four-quark operator basis of the case of MSSM from 8 to 28, but also introduce new, likely to be dominating, contributions in the form of charged-slepton and sneutrino loops to the Wilson coefficients of (chromo)magnetic penguins. However, our results clearly show that the new four-quark operators with non-vanishing Wilson coefficients at the electroweak/SUSY scale, induce effects through QCD running which typically dominate over the direct contributions to the Wilson coefficients of (chromo)magnetic penguins. However, there are exceptions. Depending on the particles exchanged, the loop contributions could also dominate in some cases.

The two-λ' type of RPV contributions split into two classes: (A) $\lambda'_{i3j}\lambda'^{*}_{h2k}$ and (B) $\lambda'^{*}_{ij3}\lambda'_{hk2}$. Whereas the contributions in class (A) give rise to $b_{_R}\to s_{_L}$ transition and hence in direct interference with major contributions from SM and R-parity conserving SUSY parts, the contributions in class (B) have not much R-parity conserving counterparts. We obtain numerical bounds, some cases of which are orders of magnitude stronger than available bounds in the literature. The interpretation of such bounds has to be taken more carefully. Their values depend strongly on the choice of other SUSY parameters. Moreover, it could happen that the R-parity conserving and RPV contributions have some accidental, but strong cancellation. In the latter case, no meaningful bounds on the RPV couplings alone can be obtained. After all, the extra contributions in the case of MSSM are expected to have partial cancellations to offset the strong charged Higgs contribution. Our numerical results at least indicate clearly the strong implication of RPV couplings on $b\to s+\gamma$ at a level substantially beyond earlier studies are able to illustrate. A most conservative

interpretation of the bounds obtained would be that they indicate values of the λ'-couplings around and above which the corresponding RPV contribution alone to $b \to s + \gamma$ would be of alarming magnitude. We also explain clearly why the λ''-couplings have no major role to play in $b \to s + \gamma$. Another type of significant contributions come from combinations of a bilinear and a trilinear RPV couplings. The type of contributions has a quite different structure and has not been studied before. They are implicitly included in our comprehensive formulation presented here, while the relevant numerical study is to be presented in another publication[24].

All the discussions above, like most of the earlier studies, has not taken into consideration constraints on the RPV parameters from the neutrino masses. However, taking the reasonable assumption that all the neutrino masses are in the sub-eV range, and that there are no strong cancellations among RPV contributions, very stringent constraints on the parameters can be obtained [36, 37, 38, 39]. In fact, such constraints are so important that talking about other numerical constraints on RPV parameters without reference to the neutrino mass constraints may not be a sensible way to take the model seriously. So, we would like to comment on the issue here. Majorana neutrino masses could be induced at one loop level by a pair of trilinear RPV couplings $\lambda'_{ilm}\lambda'_{jml}$. Because these violate lepton number by two units, they cannot contribute to the decay $b \to s + \gamma$. However, the case $l = m$ could be used to obtain bounds on λ'_{imm}. Strong bounds on such individual couplings could significantly strengthen the bounds on some of the combinations that contribute to $b \to s + \gamma$. For instance, choosing the spectrum similar to the one for this study, one obtains a strong upper bound of $|\lambda'_{i33}| = 7.1 \times 10^{-4}$. The bound on the parameter λ'_{i22} is much less stringent ($|\lambda'_{i22}| = 3.0 \times 10^{-2}$) as it is suppressed by a quadratic factor of $(m_s/m_b)^2$ relative to the one-loop contribution from the parameter λ'_{i33}. This would mean that, whenever the coupling λ'_{imm} is a part of the combination contributing to $b \to s + \gamma$, bounds coming from neutrino mass consideration are stronger. Nevertheless, the bounds obtained by us on three combinations in case (B), namely $|\lambda'_{131}\lambda'_{121}|, |\lambda'_{231}\lambda'_{221}|, |\lambda'_{331}\lambda'_{321}|$, still survive because λ'_{imm} does not figure in these combinations.

note added in proof: Just after this work was finished, an eprint [40] appeared, where the branching fraction for $B \to X_s + \gamma$ has been recalculated at the NLL order using the results of soft-collinear factorization for inclusive B-meson decay distributions. It has been pointed out that the singnificant perturbative uncertainties associated with the parameter $\Delta = m_b - 2E_0$ have been ignored in the previous works. The new estimate now stands at $Br\left[B \to X_s + \gamma\ (E_\gamma > 1.8GeV)\right]_{\rm SM} = (3.44 \pm 0.53 \pm 0.35) \times 10^{-4}$, where the first error is the estimate of perturbative uncertainties and the second one reflects uncertainties in the input parameters. As a result of this larger theoretical uncertainties, the lower bound on the charged-Higgs mass is strongly reduced compared to previous estimates, to slightly below 200 GeV at 95 % confidence level. With the larger theoretical uncertainties in the SM prediction, the case for new physics certainly becomes stronger.

Acknowledgment: O.K. thanks the Institute of Physics, Academia Sinica, Taiwan for hospitality during the early phase of the work. R.V. acknowledges the hospitality of the Korea Institute for Advanced Study (KIAS), Korea and KEK, Japan, during his visit where a part of the manuscript was written. We also thank E.J.Chun, H.-N.Li, K. Hagiwara and K.S.Babu for the useful discussions and N.Oshimo for the correspondence. Our work is partially supported by research grants from the National Science Council of Taiwan. O.K. is supported under grant number NSC 92-2112-M-008-044 and NSC 91-2112-M-008-042. R.V. is supported under post-doc grant number NSC 92-2811-M-008-012 and NSC 92-2811-M-008-003.

APPENDIX A: THE γ MATRIX

In table II,III we provide a translation of our notation of operators to that of refs.[20, 21] for easy comparison. We define the scheme independent anomalous dimension matrix $\hat{\gamma}^{\rm eff}$ as:

$$\hat{\gamma}^{(0)\rm eff} = \begin{pmatrix} \gamma_L^{\rm eff} & 0 \\ 0 & \gamma_R^{\rm eff} \end{pmatrix} \tag{A1}$$

where $\gamma_L^{\rm eff}$ and $\gamma_R^{\rm eff}$ are given as (for convenience we have given the operators on the top row):

$$\gamma_L^{\rm eff} = \begin{array}{c} \begin{array}{cccccccccccc} \mathcal{Q}_1 & \mathcal{Q}_2 & \mathcal{Q}_3 & \mathcal{Q}_4 & \mathcal{Q}_5 & \mathcal{Q}_6 & \mathcal{Q}_7 & \mathcal{Q}_8 & \mathcal{Q}_9 & \mathcal{Q}_{10} & \mathcal{Q}_{11} \end{array} \\ \left(\begin{array}{cccccccccccc} -2 & 6 & 0 & 0 & 0 & 0 & 0 & 3 & 0 & 0 & 0 \\ 6 & -2 & -\frac{2}{9} & \frac{2}{3} & -\frac{2}{9} & \frac{2}{3} & \frac{416}{81} & \frac{70}{27} & 0 & 0 & 0 \\ 0 & 0 & -\frac{22}{9} & \frac{22}{3} & -\frac{4}{9} & \frac{4}{3} & -\frac{464}{81} & \frac{545}{27} & 0 & 0 & 0 \\ 0 & 0 & \frac{44}{9} & \frac{4}{3} & -\frac{10}{9} & \frac{10}{3} & \frac{136}{81} & \frac{512}{27} & 0 & 0 & 0 \\ 0 & 0 & 0 & 0 & 2 & -6 & \frac{32}{9} & \frac{-59}{3} & 0 & 0 & 0 \\ 0 & 0 & -\frac{10}{9} & \frac{10}{3} & -\frac{10}{9} & -\frac{38}{3} & -\frac{296}{81} & -\frac{703}{27} & 0 & 0 & 0 \\ 0 & 0 & 0 & 0 & 0 & 0 & \frac{32}{3} & 0 & 0 & 0 & 0 \\ 0 & 0 & 0 & 0 & 0 & 0 & -\frac{32}{9} & \frac{28}{3} & 0 & 0 & 0 \\ 0 & 0 & -\frac{2}{9} & \frac{2}{3} & -\frac{2}{9} & \frac{2}{3} & \frac{200}{81} & -\frac{119}{27} & -16 & 0 & 0 \\ 0 & 0 & -\frac{2}{9} & \frac{2}{3} & -\frac{2}{9} & \frac{2}{3} & \frac{200}{81} & -\frac{119}{27} & 0 & -16 & 0 \\ 0 & 0 & -\frac{2}{9} & \frac{2}{3} & -\frac{2}{9} & \frac{2}{3} & \frac{200}{81} & -\frac{227}{27} & 0 & 0 & -16 \end{array} \right) \end{array} \tag{A2}$$

$$\gamma_R^{\rm eff} = \begin{array}{c} \begin{array}{ccccccccccccccccc} \widetilde{\mathcal{Q}}_1 & \widetilde{\mathcal{Q}}_2 & \widetilde{\mathcal{Q}}_3 & \widetilde{\mathcal{Q}}_4 & \widetilde{\mathcal{Q}}_5 & \widetilde{\mathcal{Q}}_6 & \widetilde{\mathcal{Q}}_7 & \widetilde{\mathcal{Q}}_8 & \widetilde{\mathcal{Q}}_9 & \widetilde{\mathcal{Q}}_{10} & \widetilde{\mathcal{Q}}_{11} & \widetilde{\mathcal{Q}}_{12} & \widetilde{\mathcal{Q}}_{13} & \widetilde{\mathcal{Q}}_{14} & \widetilde{\mathcal{Q}}_{15} & \widetilde{\mathcal{Q}}_{16} & \widetilde{\mathcal{Q}}_{17} \end{array} \\ \left(\begin{array}{ccccccccccccccccc} -2 & 6 & 0 & 0 & 0 & 0 & 0 & 3 & 0 & 0 & 0 & 0 & 0 & 0 & 0 & 0 & 0 \\ 6 & -2 & -\frac{2}{9} & \frac{2}{3} & -\frac{2}{9} & \frac{2}{3} & \frac{416}{81} & \frac{70}{27} & 0 & 0 & 0 & 0 & 0 & 0 & 0 & 0 & 0 \\ 0 & 0 & -\frac{22}{9} & \frac{22}{3} & -\frac{4}{9} & \frac{4}{3} & -\frac{464}{81} & \frac{545}{27} & 0 & 0 & 0 & 0 & 0 & 0 & 0 & 0 & 0 \\ 0 & 0 & \frac{44}{9} & \frac{4}{3} & -\frac{10}{9} & \frac{10}{3} & \frac{136}{81} & \frac{512}{27} & 0 & 0 & 0 & 0 & 0 & 0 & 0 & 0 & 0 \\ 0 & 0 & 0 & 0 & 2 & -6 & \frac{39}{9} & -\frac{59}{3} & 0 & 0 & 0 & 0 & 0 & 0 & 0 & 0 & 0 \\ 0 & 0 & -\frac{10}{9} & \frac{10}{3} & -\frac{10}{9} & -\frac{38}{3} & -\frac{296}{81} & -\frac{703}{27} & 0 & 0 & 0 & 0 & 0 & 0 & 0 & 0 & 0 \\ 0 & 0 & 0 & 0 & 0 & 0 & \frac{32}{3} & 0 & 0 & 0 & 0 & 0 & 0 & 0 & 0 & 0 & 0 \\ 0 & 0 & 0 & 0 & 0 & 0 & -\frac{32}{9} & \frac{28}{3} & 0 & 0 & 0 & 0 & 0 & 0 & 0 & 0 & 0 \\ 0 & 0 & -\frac{2}{9} & \frac{2}{3} & -\frac{2}{9} & \frac{2}{3} & \frac{200}{81} & -\frac{119}{27} & -16 & 0 & 0 & 0 & 0 & 0 & 0 & 0 & 0 \\ 0 & 0 & -\frac{2}{9} & \frac{2}{3} & -\frac{2}{9} & \frac{2}{3} & \frac{200}{81} & -\frac{119}{27} & 0 & -16 & 0 & 0 & 0 & 0 & 0 & 0 & 0 \\ 0 & 0 & -\frac{2}{9} & \frac{2}{3} & -\frac{2}{9} & \frac{2}{3} & \frac{200}{81} & -\frac{227}{27} & 0 & 0 & -16 & 0 & 0 & 0 & 0 & 0 & 0 \\ 0 & 0 & -\frac{2}{9} & \frac{2}{3} & -\frac{2}{9} & \frac{2}{3} & -\frac{448}{81} & -\frac{119}{27} & 0 & 0 & 0 & -16 & 0 & 0 & 0 & 0 & 0 \\ 0 & 0 & -\frac{2}{9} & \frac{2}{3} & -\frac{2}{9} & \frac{2}{3} & -\frac{448}{81} & -\frac{119}{27} & 0 & 0 & 0 & 0 & -16 & 0 & 0 & 0 & 0 \\ 0 & 0 & 0 & 0 & 0 & 0 & 0 & 3 & 0 & 0 & 0 & 0 & 0 & -2 & 6 & 0 & 0 \\ 0 & 0 & -\frac{2}{9} & \frac{2}{3} & -\frac{2}{9} & \frac{2}{3} & \frac{416}{81} & \frac{70}{27} & 0 & 0 & 0 & 0 & 0 & 6 & -2 & 0 & 0 \\ 0 & 0 & 0 & 0 & 0 & 0 & 0 & 3 & 0 & 0 & 0 & 0 & 0 & 0 & -2 & 6 & \\ 0 & 0 & -\frac{2}{9} & \frac{2}{3} & -\frac{2}{9} & \frac{2}{3} & -\frac{232}{81} & \frac{70}{27} & 0 & 0 & 0 & 0 & 0 & 0 & 6 & -2 & \end{array} \right) \end{array} \tag{A3}$$

TABLE II: Operators that mix in the block $\gamma_L^{\rm eff}$

Our notation	$\mathcal{Q}_1$	$\mathcal{Q}_2$	$\mathcal{Q}_3$	$\mathcal{Q}_4$	$\mathcal{Q}_5$	$\mathcal{Q}_6$	$\mathcal{Q}_7$	$\mathcal{Q}_8$	$\mathcal{Q}_9$	$\mathcal{Q}_{10}$	$\mathcal{Q}_{11}$
Ref.[21]	O_{1L}	O_{2L}	O_{3L}	O_{4L}	O_{5L}	O_{6L}	O_{7L}	O_{8L}	O_{6L}^d	O_{6L}^s	O_{6L}^b
Ref.[20]	O_1	O_2	O_3	O_4	O_5	O_6	O_7	O_8	P_6	P_7	P_8

[1] K. Hagiwara et.al. [Particle Data Group Collaboration], "Review of Particle Physics," Phys. Rev. **D 66** 010001 (2002).

[2] For the earlier works, see B.Grinstein *et al.* Phys. Lett. **B202** 138 (1988); R.Grigjanis *et al.* Phys. Lett. **B213** 355 (1988); M.Misiak Phys. Lett. **B269** 161 (1991), Nucl. Phys. **B393** 23 (1993); The issue of 'scheme dependence' was resolved by M.Ciuchini *et al.* Phys. Lett. **B316** 127 (1993), Nucl. Phys. **B421** 41 (1994).

TABLE III: Operators that mix in the block $\gamma_R^{\rm eff}$.

Our notation	$\widetilde{\mathcal{Q}}_1$	$\widetilde{\mathcal{Q}}_2$	$\widetilde{\mathcal{Q}}_3$	$\widetilde{\mathcal{Q}}_4$	$\widetilde{\mathcal{Q}}_5$	$\widetilde{\mathcal{Q}}_6$	$\widetilde{\mathcal{Q}}_7$	$\widetilde{\mathcal{Q}}_8$	$\widetilde{\mathcal{Q}}_9$	$\widetilde{\mathcal{Q}}_{10}$	$\widetilde{\mathcal{Q}}_{11}$	$\widetilde{\mathcal{Q}}_{12}$	$\widetilde{\mathcal{Q}}_{13}$	$\widetilde{\mathcal{Q}}_{14}$	$\widetilde{\mathcal{Q}}_{15}$	$\widetilde{\mathcal{Q}}_{16}$	$\widetilde{\mathcal{Q}}_{17}$
Ref.[21]	O_{1R}	O_{2R}	O_{3R}	O_{4R}	O_{5R}	O_{6R}	O_{7R}	O_{8R}	O_{6R}^{d}	O_{6R}^{s}	O_{6R}^{b}	O_{6R}^{u}	O_{6R}^{c}	O_{3R}^{u}	O_{4R}^{u}	O_{3R}^{d}	O_{4R}^{d}
Ref.[20]	R_3	R_4	P_9	P_{10}	P_{11}	P_{12}	$\widetilde{O}_7$	$\widetilde{O}_8$	P_3	P_4	P_5	P_1	P_2	R_1	R_2	R_5	R_6

[3] Scheme-independence was further confirmed using an unconventional scheme by G. Cella *et al.* Nucl. Phys. **B421** 417 (1994), Phys. Lett. **B325** 227 (1994).
[4] P. Gambino and M. Misiak Nucl. Phys. **B611** 01 (20338). Also see A. Kagan and M. Neubert Eur. Phys. J.C **7** 5 (1999).
[5] A. Buras *et al.* Nucl. Phys. **B631** 219 (2002).
[6] S. Chen *et al.* (CLEO Collaboration) Phys. Rev. Lett. **87** 251807 (2001).
[7] K. Abe *et al.*(BELLE Collaboration) Phys. Lett. **B511** 151 (2001).
[8] R. Barate *et al.* (ALEPH Collaboration) Phys. Lett. **B429** 169 (1998).
[9] C. Jessop, SLAC-PUB-9610.
[10] S.Bartolini *et al.* Nucl. Phys. **B353** 591 (1991); N.Oshimo Nucl. Phys. **B404** 20 (1993); F.Borzumati Z. Physik **C63** (19291) 94; G.Degrassi *et al.*JHEP 0012:009,2000. Importance of Chargino contributions was first pointed out by R. Garisto and J.Ng in Phys. Lett. **B315** 372 (1993). For further details see the recent review by T.Hurth [arXiv:hep-ph/0212304] and references therein.
[11] H.Baer *et al.* Phys. Rev. **D58** 015007 (1998).
[12] M.Carena *et al.* Phys. Lett. **B499** 141 (2001).
[13] For a pedagogic review of the formulation please see O.C.W. Kong Int.J.Mod.Phy. A19, 1863 (2004).
[14] C.D.Frogatt and H.B.Neilsen Nucl. Phys. **B47** 277 (1979).
[15] A.S.Joshipura, R.Vaidya, S.K.Vempati Phys. Rev. **D62** 093029 (2000) [arXiv:hep-ph/0006138].
[16] The preliminary results of this work were presented at the 2nd International Conference on Flavor Physics (ICFP), Korea, in Sept. 2003. Preprint NCU-HEP-k013, to appear in the Journal of Korean Physical Society (JKPS), ICFP proceedings.
[17] M. Bisset *et al.* Phys. Lett. **B430** 274 (1998); Phys. Rev. **D62** 035001 (2000).
[18] K. Cheung and O.C.W. Kong Phys. Rev. **D64** 095007 (2001).
[19] B. de Carlos and P.L. White Phys. Rev. **D55** 4222 (1997). Also see, D.Chakraverty *et al.* Phys. Rev. **D63** 075009 (2001).
[20] Th. Besmer and A. Steffen Phys. Rev. **63** 055007 (2001).
[21] E.Chun *et al.* Phys. Rev. **D62** 076006 (2000). Also see G. Bhattacharyya *et al.* Phys. Lett. **B493** 113 (2000).
[22] O.C.W. Kong JHEP **0009**, *037* (2000)
[23] Y.-Y. Keum and O.C.W. Kong Phys. Rev. Lett. **86** 393 (2001); Phys. Rev. **D63** 113012 (2001).
[24] O.C.W. Kong and R.D. Vaidya, NCU-HEP-k017, hep-ph/0408115.
[25] For a pedagogic treatment of the the formulation and the techniques, see A. Buras [arXiv:hep-ph/9806471].
[26] H.D. Politzer Nucl. Phys. **B172** 349 (1980).
[27] H.Simma Z. Physik **C61** (1967) 94.[arXiv:hep-ph/9307274].
[28] K.Chetyrkin *et al.* Phys. Lett. **B400** 206 (1997), [Erratum Phys. Lett. **B425** 97 (19414)].
[29] F. Borzumati *et al.* Phys. Rev. **D62** 075005 (2000) [arXiv: hep-ph/9911245].
[30] K.I. Okamura and L. Roszkowski JHEP 0310:024,2003 [arXiv: hep-ph/0308102].
[31] A.Buras *et al.* Nucl. Phys. **B424** 374 (1994).
[32] S. Ferrara and E. Remiddi Phys. Lett. **B53** 347 (1974).
[33] G. F. Guidichi *et al.* Nucl. Phys. **B645** 155 (2002) [arXiv:hep-ph/0207036].
[34] T. Besmer *et al.* Nucl. Phys. **B609** 359 (2001) [arXiv:hep-ph/0105292].
[35] M.Chemtob [arXiv:hep-ph/0406029]. Also see G.Bhattacharya Nucl. Phys. B (Proc. Suppl.) **52A** 83 (1997); B.Allanach *et al.* Phys. Rev. **D60** 075014 (1999).
[36] For the structure of the λ'-couplings induced neutrino masses, see for example O.C.W.Kong, Mod.Phys.Lett. **A 14**,903 (1999) and references therein.
[37] See S.K.Kang and O.C.W.Kong, Phys. Rev. **D69** 013004 (2004).
[38] A.S.Joshipura, R.D.Vaidya and S.K.Vempati, Phys. Rev. **D65** 053018 (1902); Nucl. Phys. **B639** 290 (2002).
[39] K.Cheung and O.C.W.Kong, Phys. Rev. **D61** 113012 (2000).
[40] M. Neubert hep-ph/0408179.